AD-A047 916 NAVAL OCEAN SYSTEMS CENTER SAN DIEGO CALIF F/G 17/2.1
APPLICATION OF A ROOT FINDING METHOD FOR TROPOSPHERIC DUCTING P--ETC(U)
SEP 77 C L GOODHART, R A PAPPERT
UNCLASSIFIED NOSC/TR-153 NL

END
DATE FILMED
1-78
DDC

(12)

NOSC

NOSC / TR 153

Technical Report 153

APPLICATION OF A ROOT FINDING METHOD FOR TROPOSPHERIC DUCTING PRODUCED BY TRILINEAR REFRACTIVITY PROFILES

CL Goodhart (Megatek Corporation) and RA Pappert (NOSC)

12 September 1977

Research 30 September 1976 through 30 September 1977

Prepared for
Office of Naval Research

NAVAL OCEAN SYSTEMS CENTER
SAN DIEGO, CALIFORNIA 92152

NAVAL OCEAN SYSTEMS CENTER, SAN DIEGO, CA 92152

AN ACTIVITY OF THE NAVAL MATERIAL COMMAND

RR GAVAZZI, CAPT USN
Commander

HL BLOOD
Technical Director

ADMINISTRATIVE INFORMATION

Work was done under 61153N, RR02101, RR0210101 (NOSC M103), by the Tropospheric Assessment Systems Branch over the period 30 September 1976 through 30 September 1977. The report was approved for publication 12 September 1977.

The authors acknowledge the beneficial suggestions offered by CH Shellman, who developed the RFM, during the course of this study.

Released by
JH Richter, Head
EM Propagation Division

Under authority of
JD Hightower, Head
Environmental Sciences Department

(14) NOSC/TR-153

UNCLASSIFIED

SECURITY CLASSIFICATION OF THIS PAGE (When Data Entered)

REPORT DOCUMENTATION PAGE	READ INSTRUCTIONS BEFORE COMPLETING FORM
1. REPORT NUMBER: NOSC Technical Report 153 (TR 153) ✓ 2. GOVT ACCESSION NO.	3. RECIPIENT'S CATALOG NUMBER
4. TITLE (and Subtitle): (6) APPLICATION OF A ROOT FINDING METHOD FOR TROPOSPHERIC DUCTING PRODUCED BY TRILINEAR REFRACTIVITY PROFILES	5. TYPE OF REPORT & PERIOD COVERED
	6. PERFORMING ORG. REPORT NUMBER
7. AUTHOR(s): (10) CL Goodhart (Megatek Corporation) and RA Pappert (NOSC)	8. CONTRACT OR GRANT NUMBER(s)
9. PERFORMING ORGANIZATION NAME AND ADDRESS: Naval Ocean Systems Center, San Diego, California 92152 ✓	10. PROGRAM ELEMENT, PROJECT, TASK AREA & WORK UNIT NUMBERS: 61153N, RR02101, RR0210101 (NOSC M103)
11. CONTROLLING OFFICE NAME AND ADDRESS: Office of Naval Research (ONR 427), Arlington, VA 22217	12. REPORT DATE: (11) 12 Sept 1977
	13. NUMBER OF PAGES: 50 (12) 54 p.
14. MONITORING AGENCY NAME & ADDRESS (if different from Controlling Office)	15. SECURITY CLASS. (of this report): Unclassified
	15a. DECLASSIFICATION/DOWNGRADING SCHEDULE
16. DISTRIBUTION STATEMENT (of this Report): Approved for public release; distribution is unlimited	
(9) Technical rept. 30 Sep 76-30 Sep 77	
17. DISTRIBUTION STATEMENT (of the abstract entered in Block 20, if different from Report)	
(16) RR02101 (17) RR0210101	
18. SUPPLEMENTARY NOTES: 393 159	
19. KEY WORDS (Continue on reverse side if necessary and identify by block number): Ducting; Electronic warfare; Propagation; Refraction; Telecommunications	

DDC RECEIVED DEC 23 1977 F

20. ABSTRACT (Continue on reverse side if necessary and identify by block number)

Knowledge of whether or not all modes of consequence have been found is of paramount importance in numerical waveguide studies. A general root finding method (RFM), developed for vlf/lf propagation in the earth-ionosphere waveguide, locates all complex zeros in physically important rectangular regions of the complex plane. The method, based on phase contour tracing, is applied to the problem of tropospheric ducting in a trilinear refractivity environment. Frequencies from vhf and into the microwave range are considered. Principles upon which the RFM is founded are reviewed and modifications of the modal equation demanded by the method are discussed. Particularly in the microwave range, overflow can be a problem and methods of overcoming this are

Next page

DD FORM 1 JAN 73 1473 EDITION OF 1 NOV 65 IS OBSOLETE S/N 0102 LF 014 6601

UNCLASSIFIED

SECURITY CLASSIFICATION OF THIS PAGE (When Data Entered)

20. Abstract. (continued)

discussed. However, the RFM is most easily implemented if the latter modifications can be avoided. Therefore, tables are included to indicate for trilinear profiles the maximum frequency below which no overflow problems would occur. These tables depend upon the maximum number which the computer can handle, the location of the search rectangle, and the refractivity profile parameters. In the present case study of ducting produced by a strong elevated layer (40 M unit deficit at about 200 m) the RFM has been applied successfully into S band with computer run time requirements comparable to those of the more conventional Newton-Raphson method.

OBJECTIVE

Explore the utility of a recently developed root finding method (RFM) for locating waveguide modal solutions associated with tropospheric ducting produced by trilinear refractivity environments.

RESULTS

In the present case study of ducting produced by a strong elevated layer (40 M unit deficit at about 200 m) the RFM has been applied successfully from vhf into S band with computer run time requirements comparable to those of the more conventional Newton-Raphson method. The RFM, however, unlike the Newton-Raphson method, assures the location of all significant modes.

RECOMMENDATION

Investigate the utility of the RFM for locating modes in multisegmented tropospheric refractivity environments.

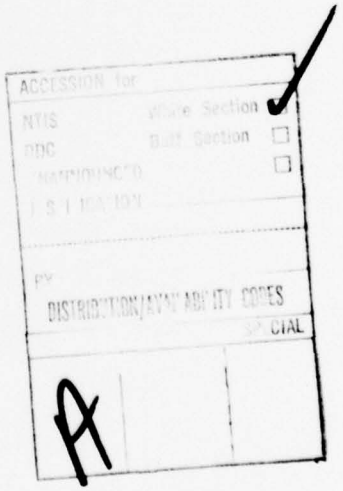

CONTENTS

1. INTRODUCTION

It is well known that the presence of strong gradient, layered structure of the troposphere greatly influences the propagation of radio waves of frequency greater than 30 MHz (and perhaps lower under strong layering conditions) to the extent that beyond the horizon ducted fields may be many tens of dB above the troposcatter fields. It has been recognized for a long time that waveguide concepts can be used to at least qualitatively explain much anomalous propagation and with the advent of the modern day computer a number of rather recent studies[1-6] have been concerned with rather detailed calculations in tropospheric ducting environments based on waveguide concepts. Waveguide theory treats the field as being composed of one or more discrete families (modes) of plane waves confined to a waveguide which, in the case of tropospheric ducts, has an upper boundary that can vary between tens of metres and thousands of metres. The number of waveguide modes needed to adequately represent the field for tropospheric ducts produced by elevated layers can typically range from one mode at the lower end of the vhf band to hundreds of modes at S band. The propagation parameters (ie, phase velocities and attenuation rates) depend upon the geometry of the guide and principally upon the tropospheric refractivity (or refractive index) profile. For a horizontally stratified guide, once all significant modes have been found, the radio fields can be determined for a given transmitter-receiver configuration by simply summing (with proper weights) the significant modes.

Unfortunately, for realistic layered refractivity profiles, solutions to the modal equation cannot be found explicitly but rather must be found by iterative techniques so that a crucial problem in numerical waveguide studies is knowing whether or not all modes of consequence have been found. Mathematically this reduces to the problem of finding the complex zeros of a modal equation in some region of a complex eigenvalue space. A quotation from Hamming[7] concerning the problem of locating complex zeros of a function seems appropriate at this point.

> "It is curious that the real-zero problem has been extensively investigated while the complex-zero problem has generally been ignored. Evidently it is a field ripe for further research."

One recent root finding method[8] (RFM) developed primarily for vlf and lower lf (10 kHz to about 60 kHz) propagation in the earth-ionosphere waveguide finds all modes in

---

1. Wait, JR, and Spies, KP, Internal guiding of microwaves by an elevated tropospheric layer, Radio Sci vol 4, 1969, p 319-326
2. Chang, HT, The effect of tropospheric layer structures on long range VHF radio propagation, IEEE Trans Antennas Propagat, AP19, 751-756
3. Dresp, MR, Radio wave propagation in the presence of an elevated tropospheric duct, PhD Thesis (1972) University of Pennsylvania, Philadelphia, Pennsylvania
4. Dresp, MR, Tropospheric duct propagation at VHF, UHF and SHF, Mitre Corporation Technical Report MTR-3114, vol 1, October 1975
5. Pappert RA, and Goodhart, CL, Case studies of beyond-the-horizon propagation in tropospheric ducting environments, Radio Sci, vol 12, 1977, p 75-87
6. CHO, SH, and Wait, JR, EM Wave propagation in a laterally nonuniform troposphere, Cooperative Institute for Research in Environmental Sciences (CIRES), University of Colorado, EM Report 1, June 15, 1977
7. Hamming, RW, Numerical Methods for Scientists and Engineers, McGraw-Hill (Second Edition), McGraw-Hill, New York, 1973
8. Morfitt, DG, and Shellman, CH, "MODESRCH" an improved computer program for obtaining ELF/VLF/LF mode constants in an earth-ionosphere waveguide. Naval Electronics Laboratory Center interim report 77T prepared for the Defense Nuclear Agency (DNA), 1 October 1976

any physically important rectangular region of the complex eigenvalue space. In this report the utility of the RFM for finding modes associated with tropospheric ducts over the frequency range from VHF to S band will be examined. Comparisons, particularly in regard to computer time and ease of implementation, will be made with the more conventional Newton-Raphson scheme which has formed the basis for the previous tropospheric waveguide calculations presented in references 1 through 6. These comparisons will be made for a ground-based duct produced by an elevated layer between about 183m and 305m which is characterized by a refractivity deficit of about 40. The layer structure appropriate to this ground-based duct is approximated by a trilinear model. In each linear layer the basic field solutions are expressible in terms of modified Hankel functions of order one-third and their derivatives as defined by the staff of the Computation Laboratory.[9] These functions are linearly related to Airy functions. It should be appreciated that the RFM developed in reference 8 is really quite a general complex root finder and that in the present study it is being applied to a very specialized problem area.

In the following section notation for some of the more important symbols is given. In section 3 some results of complex variable theory, useful for an understanding of phase contours and their general behavior, are presented. In section 4 an abbreviated description of the RFM is given. For a more complete discussion of the latter, the interested reader is referred to reference 8. A summary of the mode equation, along with modifications demanded by the RFM, will be found in section 5. Appendix A is a mathematical supplement to section 5. Results are presented in section 6 and conclusions briefly summarized in section 7.

9. Computation Laboratory, Tables of the Modified Hankel Functions of Order One Third and Their Directives, Harvard University Press, Cambridge, Massachusetts, 1945

2. NOTATION

Figure 1 shows a typical elevated layer structure with altitude as ordinate and $(2n-1)$ as abscissa with n the modified refractive index (ie, earth curvature included). The linear regions are denoted by 1 through 3 and the trilinear model serves as the basis for the study reported here. MKS units are used throughout the study and some of the more important symbols used are the following:

x, y, z	Cartesian coordinates; z is measured vertically upwards, and x is measured horizontally in the plane of incidence
ω	$2\pi \times$ frequency of rf wave
$\mathfrak{f}$	Original modal equation
F_i	i = 1, 2, 3, 4 represents pole-free discontinuous version of modal equation
M_i	i = 1, 2, 3, 4 represents pole-free continuous version of modal equation
R_D	Plane wave reflection coefficient from everything above height D in the duct
R_D	Plane wave reflection coefficient from everything below height D in the duct
θ	Complement of the angle of incidence
s	$\sin\theta$
c	$\cos\theta$
k	Free space wave number
H	Height where modified index of refraction is taken equal to unity. H will always be taken in region 1 (see figure 1)
$p_1(N)$	Argument of Hankel function at lower boundary of region N (see figure 1)
$p_2(N)$	Argument of Hankel function at upper boundary of region N (see figure 1)

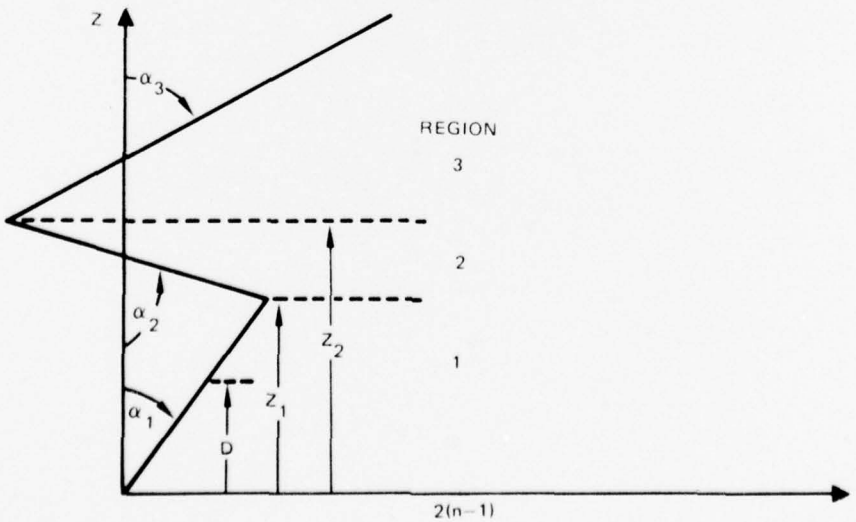

Figure 1. Schematic of trilinear model (n is the modified refractive index referenced to unity at the ground).

$p_D^{(1)}$	Argument of Hankel function at height D in region 1
α_i	i = 1, 2, 3. Slopes defined in figure 1 such that α_1 and $\alpha_3 > 0$ and $\alpha_2 < 0$
i	$\sqrt{-1}$
$h_{1,2}$	Hankel functions of order one-third as defined by Computation Laboratory[9]
$h'_{1,2}$	Derivatives of Hankel functions of order one-third as defined by Computation Laboratory[9]
r_f	Fresnel reflection coefficient for the ground for TE polarization
η	Surface rms bump height
σ	Ground conductivity
ϵ	Ground permittivity
ϵ_o	Free space permittivity
t	Time
β	A constant equal to 0.853667218838951
Im	Imaginary part of
Re	Real part of
G	Function of a complex variable which is analytic everywhere except at a finite number of isolated poles
w	A complex variable

3. A BRIEF INTRODUCTION TO PHASE CONTOURS

For understanding much of the material presented in this report it is desirable that the reader have at least a rudimentary understanding of phase contours and their general behavior for functions of a complex variable which are analytic everywhere except at isolated poles. This section is intended to serve that purpose. The objective is not to present proofs or theorems, but to impart briefly the requisite background for understanding the topology of phase contours.

Let G(w) be a function of a complex variable which is analytic everywhere except at isolated poles. The phase of G(w) is defined as arg G(w) = $\tan^{-1}$ Im (G)/Re(G). With allowance for the sign of Im(G) and Re(G) this phase is single valued in the interval $0^\circ \leq \arg G < 360^\circ$ except at a zero or pole of the function where the phase is undetermined. Expansion of such a function about any simple zero, w_0, of the function provides some insight into the phase behavior of the function. Assuming that w is close to w_0, expansion to first order is sufficient and

$$G(w) = G(w_0) + G'(w)\,(w - w_0)$$

$$= |G'(w_0)|\, e^{i\beta 0}\, |\Delta w|\, e^{i\phi} \; ; \; \Delta w = w - w_0$$

$$= |G'(w_0)\,\Delta w|\, e^{i(\beta_0 + \phi)} \qquad (1)$$

Polar notation has been employed and β_0 is a constant; namely, the phase of G(w) at w_0 while ϕ is the phase of $w - w_0$ as illustrated in figure 2(a). This indicates that near a simple zero of G(w) the phase of G(w) varies linearly with ϕ and thus increases in a counterclockwise sense about the zero. This leads to the phase diagram in figure 2(b). A set of lines of constant phase (hereafter referred to as phase contours) ranging from 0 to 2π radians emanates radially (solid lines) from a simple zero. The dashed lines depict possible phase contour behavior, in the region beyond the neighborhood of w_0, in order to emphasize that in this region the phase contours are generally not radial. In view of the phase behavior near a zero of G(w) it is conceptually useful to define a zero of G(w) as a "source" of a set of phase contours. For an n^{th} order zero the expansion of G(w) leads to similar phase behavior in the neighborhood of the zero with the exception that the phase of G(w) varies linearly with $n\phi$. It is also true that the phase change of G(w) around a counterclockwise contour enclosing an n^{th} order zero of G(w) is $2n\pi$.

The phase behavior of G(w) near a pole, w_p, of G(w) can be obtained by examining the Laurent expansion of G(w) about w_p. Using a simple pole as an example, the Laurent series is given by

$$G(w) = \sum_{n=-1}^{\infty} a_n (w - w_p)^n \; .$$

Assuming that w is close to w_p, a single term is sufficient and

$$G(w) = \frac{a_{-1}}{w - w_p} = |a_{-1}|\, e^{i\beta_{-1}}\, |\Delta w|^{-1}\, e^{-i\phi} \; ; \quad \Delta w = w - w_p$$

$$= \left|\frac{a_{-1}}{\Delta w}\right| e^{i(\beta_{-1} - \phi)} \qquad (2)$$

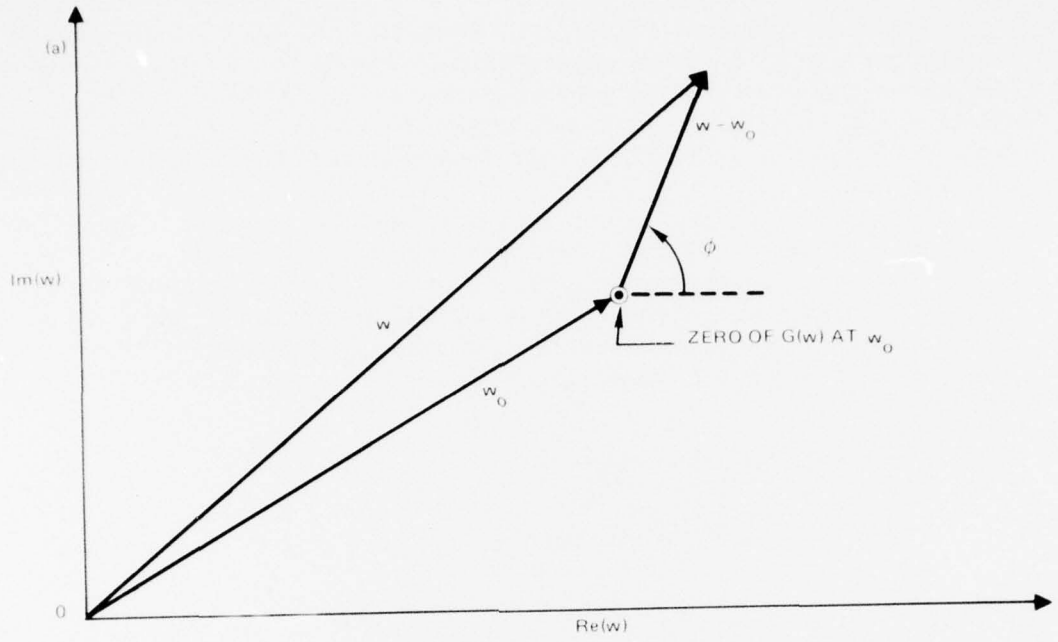

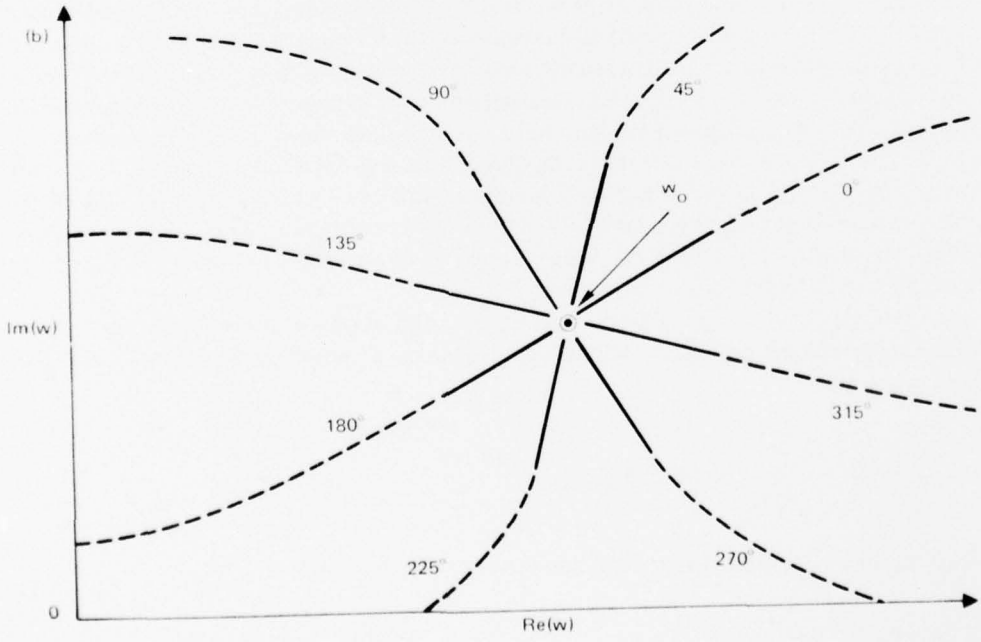

Figure 2. Phase contour behavior near a zero of G(w).
——— Phase contour in the neighborhood of w_0
– – – Phase contour beyond the neighborhood of w_0

where a_{-1} is simply a constant (a Laurent expansion coefficient), β_{-1} is also a constant equal to the phase of a_{-1}, and ϕ is the phase of $w - w_p$. Thus, near a simple pole of $G(w)$ the phase of $G(w)$ varies as $-\phi$ ($-n\phi$ for an n^{th} order pole). This leads to a phase behavior similar to that for a zero of $G(w)$, except now the phase of $G(w)$ increases in a clockwise sense about the pole as illustrated in figure 3. For reasons which will become apparent in the next section a pole is defined to be a "sink" of a set of phase contours.

A summary of the basic principles just dealt with is as follows. For a function of a complex variable which is analytic everywhere except at isolated poles:

1. Phase contours do not intersect except at zeros or poles.

2. Zeros and poles act as "sources" and "sinks," respectively, of phase contours, and the phase behavior is radial in the neighborhood of either a pole or a zero.

3. Near a zero the phase increases in a counterclockwise sense about the zero.

4. Near a pole the phase increases in a clockwise sense about the pole.

The above principles lead to the conclusion that the phase contours for a function with a single zero or pole (in the finite region of the complex plane) are simply radials extending from the zero or the pole to infinity. Of more practical interest is the phase behavior associated with a function of many zeros, of many poles, or of a mixture of the two. The phase contour behavior for such functions is dictated by two general characteristics. One characteristic is the general phase contour behavior associated with a neighboring pole and zero. The other characteristic is the general phase contour behavior associated *with two neighboring zeros* or two neighboring poles. These characteristics are illustrated by figure 4. Figure 4(a) shows phase contours for a function containing one simple zero and one simple pole. The figure illustrates the tendency for the combination of a zero and a pole to act as a "source" and a "sink" of phase contours (assignment of "source" to a zero and "sink" to a pole is arbitrary and the reverse assignment would be equally descriptive for the purposes intended here). A phase contour in such a situation is terminated on one end by a zero and on the other end by a pole. This termination of the phase contour in the finite region of the complex plane is referred to as "phase contour extinction." Figure 4(b) shows phase contours for a function of two simple zeros. The phase contour behavior is in keeping with the idea that the two zeros are both sources of phase contours. A similar situation results for two poles with the exception that the phase contours have an opposite sense of rotation about the poles. The concept of "source"-"sink" pairs is not violated here as the phase contours are terminated by the appropriate "sinks" or "sources" at infinity. One might wonder if the phase contour associated with two zeros (or poles) might ever exhibit "phase contour extinction." The suggested behavior would be that shown in figure 4(a) with the pole (or zero) replaced by a zero (or pole). It can be seen why such a case could never occur as the sense of rotation of the phase contours about one of the zeros (or poles) would be contrary to the precepts put forth in principles 3 and 4 above. Figure 4 illustrates phase contour behavior for relatively simple functions. However, as will be seen later the phase behavior of the more complicated functions of concern in this study possesses the same basic characteristics as those described above.

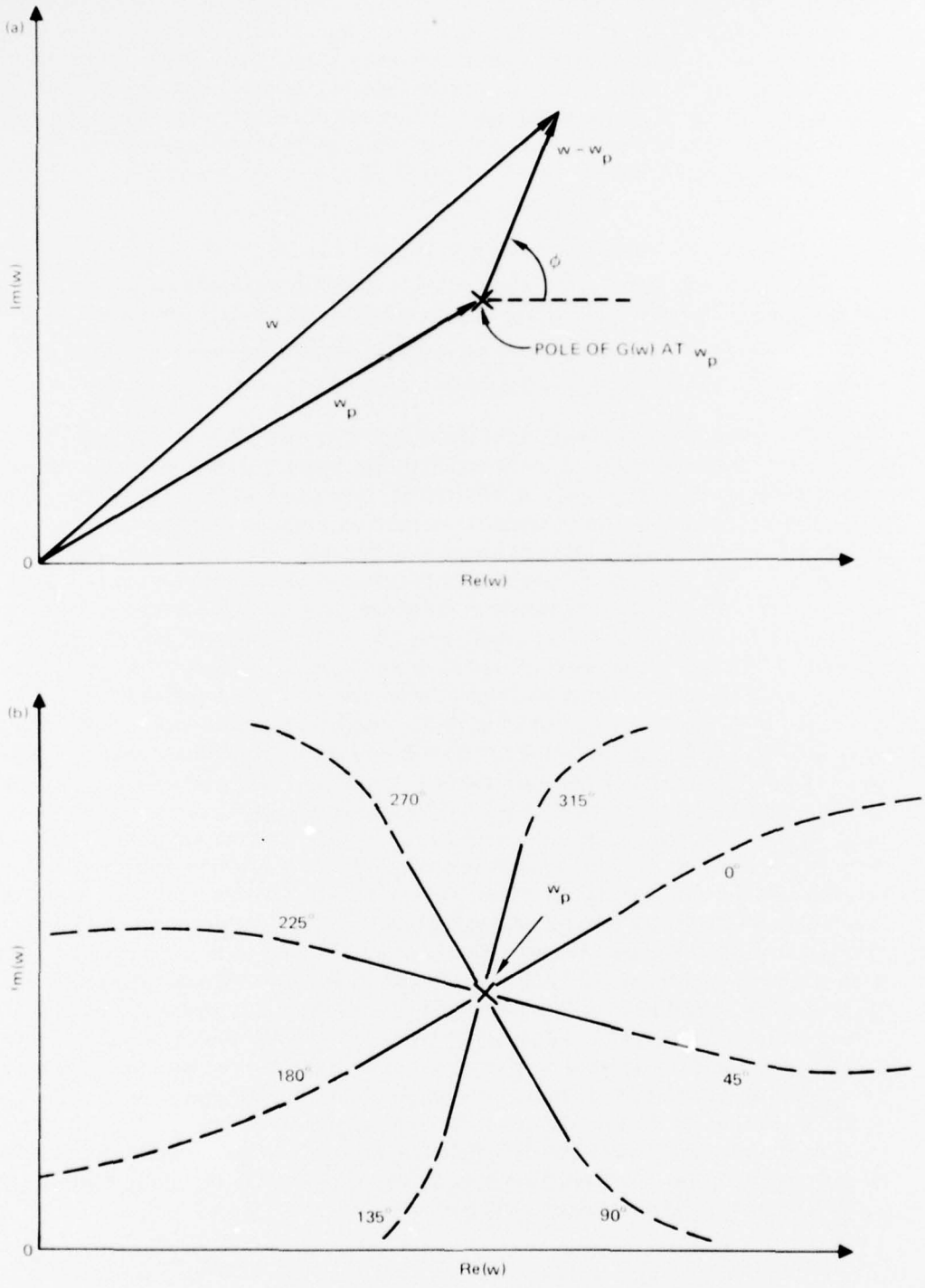

Phase 3. Phase contour behavior near a pole of G(w).
——— Phase contour in the neighborhood of w_p
– – – Phase contour beyond the neighborhood of w_p

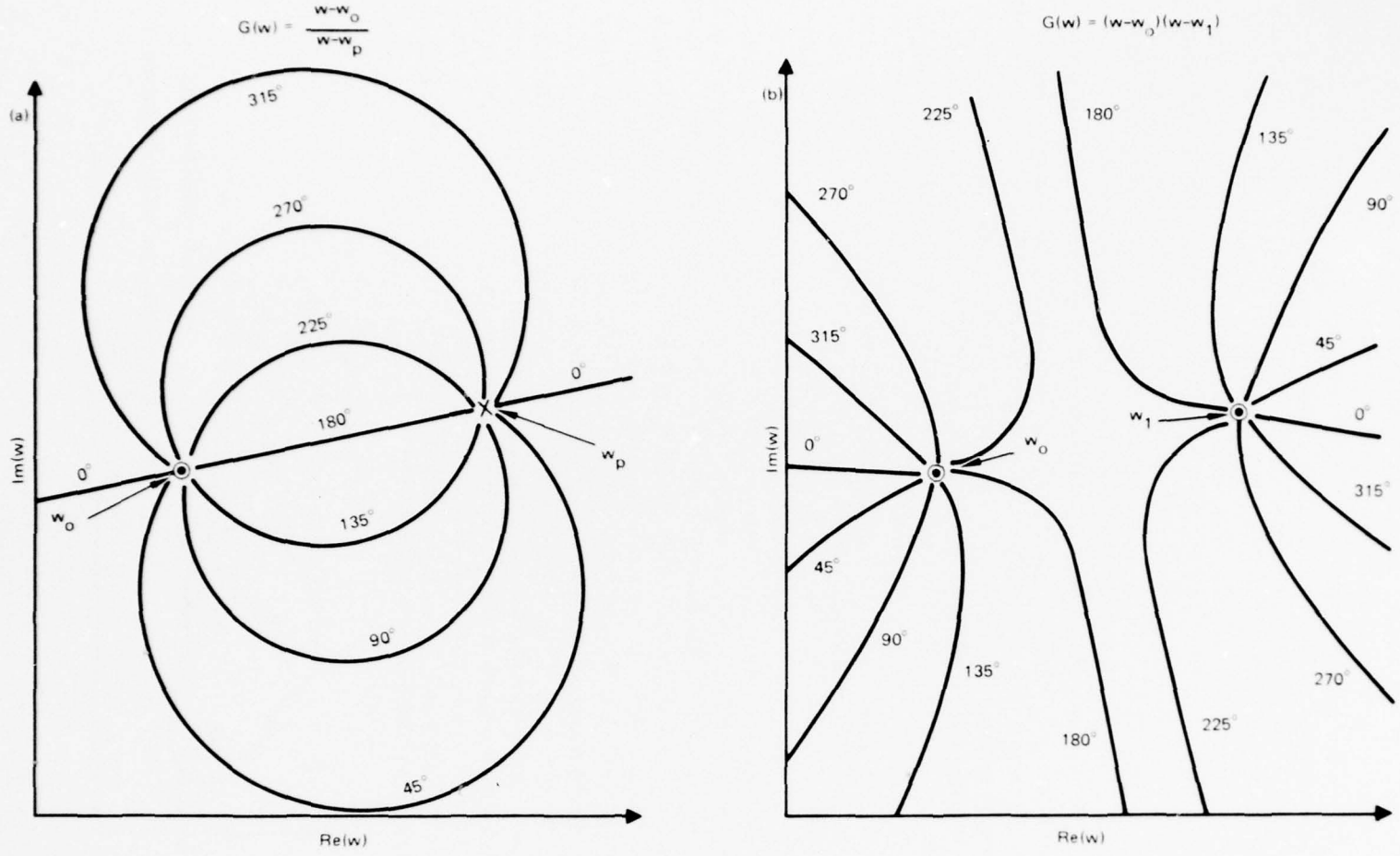

Figure 4. General phase contour behavior near zero and pole combinations for a function G(w).

4. DESCRIPTION OF THE ROOT FINDING METHOD (RFM) FOR COMPLEX ZEROS

A theorem of complex variable theory states that for a function, G(w), of a complex variable with isolated poles but otherwise analytic, the accumulated phase change of the function, around a closed counterclockwise contour, C, in the complex plane of the function argument, is equal to 2π times the number of zeros minus the number of poles enclosed by C where n^{th} order zeros and poles are counted n times (fig 5). In addition no zeros or poles may exist on C. The interested reader is referred to reference 10 for the proof of this theorem. In passing it is pointed out that this theorem suggests all the concepts discussed in the previous section. The theorem indicates that the phase change of a function, G(w), about a closed counterclockwise contour, C, enclosing only a set of n simple zeros, is equal to $2n\pi$. This directly implies that every phase contour associated with each zero crosses C. The RFM was developed from this basic principle.

Some fundamentals of the application of the RFM to find zeros of a function, G(w), are illustrated in figure 6. A search rectangle is placed about some region of the complex plane. The search rectangle is divided into a grid of mesh squares whose corners will be called mesh points. The mesh square size is optional and is usually selected according to the expected zero spacing. A mesh size that is too large can result in complications which may ultimately lead to missed zeros as will be explained in section 6. However, a mesh size that is too small leads to a costly extended computer run time. Beginning at the upper left corner of the search rectangle, a boundary search for 0° or 180° phase contours is conducted in the counterclockwise direction. Any phase contour would do; however, the 0° and 180° phase contours are selected because mathematically they are easily located, occurring when Im (G) = 0. The search is conducted by evaluating G(w) at the mesh points along the search rectangle boundary. When Im(G) changes sign, it indicates that a 0° or 180° phase contour has just been passed (points A, D, and G). Once either of these phase contours is located, the boundary search is temporarily halted while the 0° or 180° phase contour is traced into the interior of the search rectangle by inspection of Im(G) at the corners of the mesh squares (counterclockwise inspection beginning at the top left corner of each mesh square). The phase contour is followed either until a zero of G(w) is discovered (points B and E) or until the search rectangle boundary is encountered (as would be the case for the phase contour between G and H), one of which will always occur provided no poles exist in the interior of the search rectangle. When a zero is located (by means which will be explained shortly), its location is saved. Then the phase contour is traced out the opposite side of the zero,

10. Churchill, RV, Brown, JW, and Verley, RF, Complex Variables and Applications (Third edition), McGraw-Hill, New York, 1974, p 296

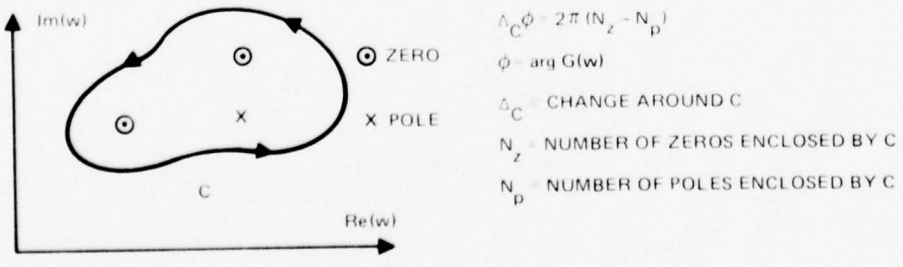

Figure 5. Phase change of a function G(w) around a closed contour.

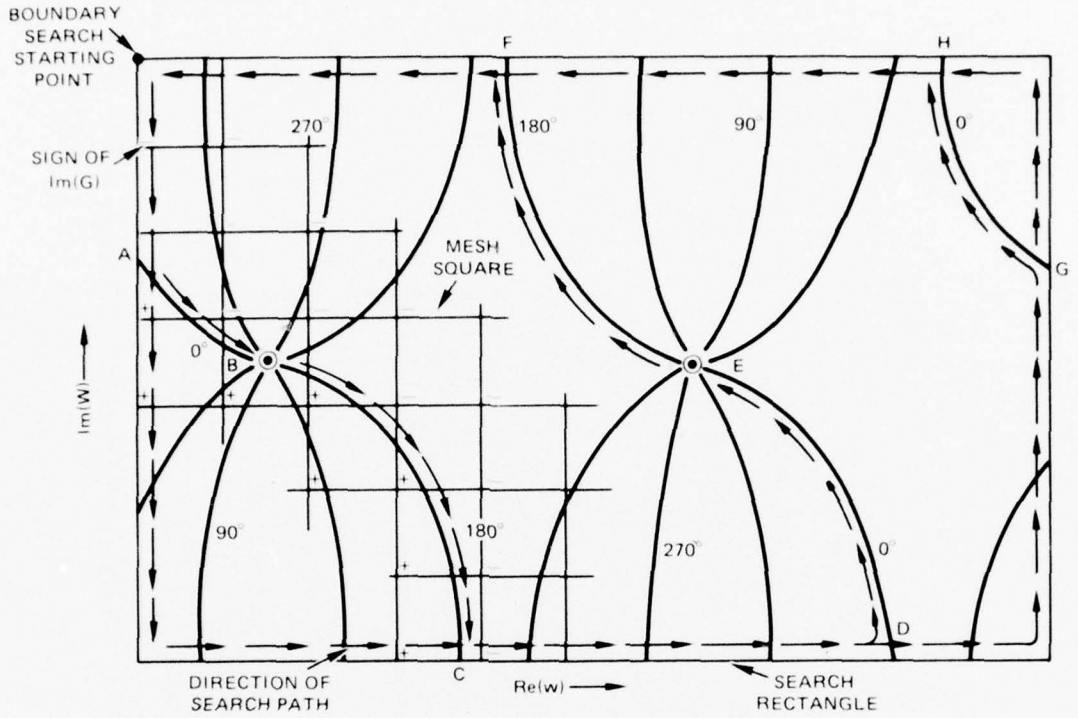

Figure 6. Root finding method (RFM) for a function G(w).
——— Phase contours for G(w)
◉ Zeros of G(w)

having undergone a 180° phase change (see fig 2(b)), until the search rectangle boundary is again encountered (points C and F). When the phase contour exits the search boundary, such as at points C, F, or H, the mesh square which contains this occurrence is flagged so as to avoid following that particular phase contour again at a later time during the boundary search. Also at such a point (point C, F or H) the phase contour trace is stopped and the boundary search is resumed at the point where the last 0° or 180° phase line was encountered (eg, points A, D, or G). Once the entire search rectangle boundary has been inspected, all the zeros of the function, G(w), located within the search rectangle will have been found.

The location of a zero is evident by the intersection of phase contours (section 3, fig 2(b)). Therefore, the intersection of the 0° or 180° phase contour with any other phase contour locates a zero of G(w). The other phase contour chosen for this purpose is the 90° or 270° phase contour, again chosen for simplicity, as these contours are easily recognized, occurring when Re(G) = 0. While a 0° or 180° phase contour is being traced, Re(G) is also examined at the corners of each mesh square to locate a Re(G) sign change which indicates that a 90° or 270° phase contour has entered the mesh square (the bold lined mesh squares in fig 7(a) and (b)). Such an occurrence indicates that a zero is probably within that mesh square (fig 7(a)) or perhaps within an adjacent mesh square (fig 7(b)). Once a mesh square is known to contain a zero, a more precise location of the zero is obtained by an interpolation scheme which employs both the magnitude and phase of the function G(w). (For details of this interpolation scheme the reader is referred to reference 8.) Following this a Newton-Raphson iteration pinpoints the location of the zero.

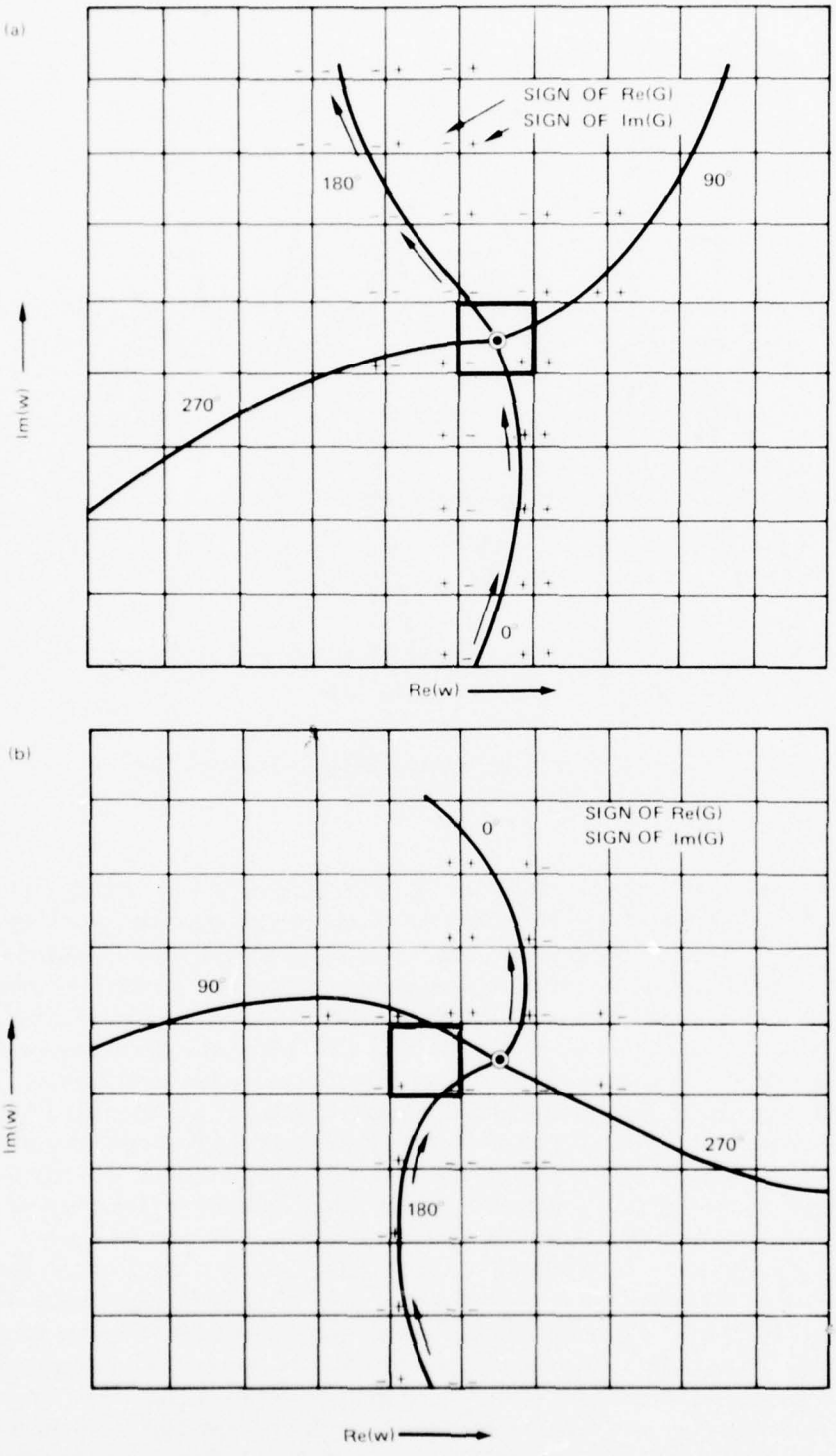

Figure 7. Locating a zero of a function G(w).
——— Phase contours for G(w)
◉ Zero of G(w)
→ Direction of search path

The RFM forbids the existence of poles in the enclosed region or on the boundary of the search rectangle. Such occurrences could lead to undetected zeros (as will be explained in section 6) due to "phase contour extinction" (see section 3, fig 4(a)). Poles may exist external to the search rectangle; but even under such restrictions if the poles are in proximity to the search rectangle, they can be a definite source of problems due to their effect on the phase contours associated with zeros that are interior to the search rectangle. This causes problems similar to those caused by the increased density of phase contours shown in figure 12 and discussed in section 6. Therefore, it is best to have a pole-free function in the finite part of the complex plane in order to assure optimum performance of the RFM. In effect, all poles should be transferred to the point infinity in the complex plane.

5. SUMMARY OF WAVEGUIDE EQUATIONS

In this section the original modal equation for the trilinear model of figure 1 along with modifications dictated by the RFM will be summarized.

The fundamental problem in planar waveguide analysis is the solution of the modal equation

$$\psi(\theta) = 1 - R_D(\theta)\, R_D(\theta) = 0 \tag{3}$$

for eigenangles, θ_n. The formulas summarized below for the plane wave reflection coefficients, R_D and R_D, are for horizontal polarization and assume a time dependence of $e^{j\omega t}$. For a derivation of the formulas the interested reader is referred to reference 11. The reflection coefficient R_D is calculated by calculating in sequence the following quantities:

$$\epsilon_2 = \frac{i\,(k/\alpha_3)^{1/3}\, h_2(p_1(3))}{h_2'(p_1(3))} = \frac{NZ2}{DZ2} \tag{4}$$

$$A(2) = \frac{i\,(|\alpha_2|/k)^{1/3}\, \epsilon_2\, h_2'(p_2(2)) - h_2(p_2(2))}{h_1(p_2(2)) - i\,(|\alpha_2|/k)^{1/3}\, \epsilon_2\, h_1'(p_2(2))} = \frac{NA2}{DA2} \tag{5}$$

$$\epsilon_1 = \frac{A(2)\, h_1(p_1(2)) + h_2(p_1(2))}{i\,(|\alpha_2|/k)^{1/3}\,(A(2)\, h_1'(p_1(2)) + h_2'(p_1(2))} = \frac{NZ1}{DZ1} \tag{6}$$

$$A(1) = \frac{-\left(i\,\epsilon_1\,(\alpha_1/k)^{1/3}\, h_2'(p_2(1)) + h_2(p_2(1))\right)}{i\,\epsilon_1\,(\alpha_1/k)^{1/3}\, h_1'(p_2(1)) + h_1(p_2(1))} = \frac{NA1}{DA1} \tag{7}$$

$$R_D = \frac{-i\,(\alpha_1/k)^{1/3}\,\left(A(1)\, h_1'(p_D(1)) + h_2'(p_D(1))\right) + s\,\left(A(1)\, h_1(p_D(1)) + h_2(p_D(1))\right)}{i\,(\alpha_1/k)^{1/3}\,\left(A(1)\, h_1'(p_D(1)) + h_2'(p_D(1))\right) + s\,\left(A(1)\, h_1'(p_D(1)) + h_2(p_D(1))\right)}$$

$$= \frac{NRD}{DRD} \tag{8}$$

The quantities $p_i(N)$ are

$$p_1(3) = (k/\alpha_3)^{2/3}\,\left(s^2 + \alpha_3\,(z_2 - z_1) + \alpha_1\,(z_1 - H)\right) \tag{9}$$

$$p_2(2) = (k/|\alpha_2|)^{2/3}\,\left(s^2 + \alpha_2\,(z_2 - z_1) + \alpha_1\,(z_1 - H)\right) \tag{10}$$

$$p_1(2) = (k/|\alpha_2|)^{2/3}\,\left(s^2 + \alpha_1\,(z_1 - H)\right) \tag{11}$$

$$p_2(1) = (k/\alpha_1)^{2/3}\,\left(s^2 + \alpha_1\,(z_1 - H)\right) \tag{12}$$

$$p_D(1) = (k/\alpha_1)^{2/3}\,\left(s^2 + \alpha_1\,(D - H)\right) \tag{13}$$

---

11. Pappert, RA, Goodhart, CL, Waveguide calculation of signal levels in tropospheric ducting environments, Naval Electronics Laboratory Center TN 3129, February 1976

Also, the quantities NZ2, NA2, NZ1, etc, are the numerators of ε_2, A2, ε_1 etc, and similarly DZ2, DA2, DZ1, etc, are the denominators of ε_2, A2, ε_1 etc.

Because the RFM requires no poles within the search rectangle and preferably none in the finite part of the complex plane (see sections 4 and 6), the modal equation requires modification as discussed subsequently. The significant point at this juncture is that the modification can lead to overflow problems if the wavefields become very evanescent or exponentially small in regions 2 or 3 (see fig 1). The overflow problems result from the quantities ε_2 and A(2) defined in equations (4) and (5), respectively. In such a circumstance, the overflows can be avoided by calculating ε_1 as follows:

$$\varepsilon_1 = \frac{h_2(p_1(2)) - e^{4\pi i/3} h_1(p_1(2))}{i(|\alpha_2|/k)^{1/3}\left(h_2'(p_1(2)) - e^{4\pi i/3} h_1'(p_1(2))\right)} = \frac{NZ1}{DZ1} \quad . \tag{14}$$

Observe that ε_2 and A(2) as defined by equations (4) and (5) now do not appear explicitly in equation (14). Thus, if the rf wave is sufficiently evanescent in regions 2 and 3, equation (14) replaces equation (6) and there is no need to calculate ε_2 and A(2) via equations (4) and (5). This is an example of what is referred to as function switching at various stages of this report. As will be discussed later, the decision to use equation (14) is based on the magnitude of the quantity L_1, which is defined as follows:

$$L_1 = \frac{2}{3}\left|\mathrm{Re}\left(i(p_1(3))^{3/2}\right)\right| + \frac{2}{3}\left|\mathrm{Re}\left(i(p_2(2))^{3/2}\right)\right| \quad . \tag{15}$$

The reflection coefficient $\bar{R}_D$ is calculated by calculating in sequence the following quantities:

$$\left.\begin{aligned} \varepsilon_0 &= \frac{1 + r_f e^{-2k^2\eta^2 s^2}}{s\left(1 - r_f e^{-2k^2\eta^2 s^2}\right)} = \frac{NZ0}{DZ0} \qquad \text{if} \qquad \mathrm{Re}(s^2) > 0 \\ &= \frac{1 + r_f}{s(1 - r_f)} = \frac{NZ0}{DZ0} \qquad \text{otherwise} \end{aligned}\right\} \tag{16}$$

$$B(1) = \frac{-(h_2(p_1(1)) + i\varepsilon_0(\alpha_1/k)^{1/3} h_2'(p_1(1))}{i\varepsilon_0(\alpha_1/k)^{1/3} h_1'(p_1(1)) + h_1(p_1(1))} = \frac{NB1}{NB2} \tag{17}$$

$$R_D = \frac{s\left(B(1)h_1(p_D(1)) + h_2(p_D(1))\right) + i(\alpha_1/k)^{1/3}\left(B(1)h_1'(p_D(1)) + h_2'(p_D(1))\right)}{-i(\alpha_1/k)^{1/3}\left(B(1)h_1'(p_D(1)) + h_2'(p_D(1))\right) + s\left(B(1)h_1(p_D(1)) + h_2(p_D(1))\right)}$$

$$= \frac{N\overline{RD}}{D\overline{RD}} \tag{18}$$

The quantity $p_1(1)$ is

$$p_1(1) = (k/\alpha_1)^{2/3}(s^2 - \alpha_1 H) \quad . \tag{19}$$

As before, NZ0, NB1, etc, denote the numerators of ε_0, B(1), etc, whereas DZ0, DB1, etc, denote their denominators.

Again, because of modifications required by the RFM, overflow problems can occur if the rf fields become very evanescent or exponentially small at the ground. In this case ground quantities can be eliminated by using the following alternative expression for R_D:

$$R_D = \frac{s\left(h_2(p_D(1)) - e^{4\pi i/3} h_1(p_D(1))\right) + i(\alpha_1/k)^{1/3}\left(h_2'(p_D(1)) - e^{4\pi i/3} h_1'(p_D(1))\right)}{s\left(h_2(p_D(1)) - e^{4\pi i/3} h_1(p_D(1))\right) - i(\alpha_1/k)^{1/3}\left(h_2'(p_D(1)) - e^{4\pi i/3} h_1'(p_D(1))\right)}$$

$$= \frac{NRD}{DKD} \tag{20}$$

The decision, as will be discussed presently, to use equation (20) instead of equation (18) is based upon the magnitude of the quantity, L_2, defined as follows:

$$L_2 = \frac{2}{3}\left|\mathrm{Re}\left(i(p_1(1))^{3/2}\right)\right| . \tag{21}$$

A rather considerable overestimate of the magnitude of the modal equation, modified so as to remove all poles to the point infinity in the complex plane is given by

$$\exp(L_1 + L_2) , \tag{22}$$

where L_1 is defined by equation (15) and L_2 by equation (21). Thus, no function switching is required if

$$L_1 + L_2 < L \tag{23}$$

where exp(L) is the maximum number the computer can handle (exp(L) will be referred to as the dynamic range of the machine). If $L_1 + L_2 > L$, the simplest decision for function switching is to use equation (14) instead of equation (6) if $L_1 > L/2$ and to use equation (20) instead of equation (18) if $L_2 > L/2$. For reasons of implementation which will become apparent later, it is a decided advantage when using the RFM to avoid function switching as much as possible. In this sense a switching scheme which better utilizes the dynamic range of the machine is indicated by the following flowchart:

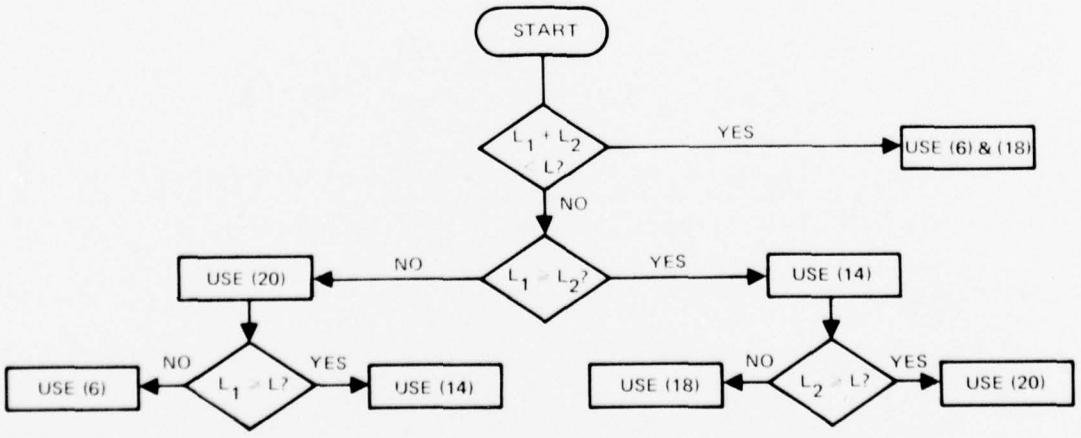

In the present study the Univac 1110 has been used with single precision format for the RFM so that the dynamic range is on the order of 10^{38} or $\cong e^{87.5}$.

As has been mentioned previously (also see sections 4 and 6), the RFM requires that there be no poles within the boundaries of the rectangular region being searched for solutions, and in fact it is preferable that all poles be transferred to the point infinity in the complex plane. Since the denominators of the preceding expressions (ie, DZ2, DA2, DZ1, etc) possess zeros, the elimination of all poles within the finite part of the complex plane can be assured by multiplying the $\mathcal{F}$ function (equation (3)) through by the denominators. Because of the switch conditions based on the parameter L (see flowchart on page 18) there are in effect four distinct representations of the modal equation. The pole-free versions of these are presented below.

Pole-Free Discontinuous Version of the Modal Equation

i) $L_1 + L_2 < L$

$$F_1 = DZ2 \times DA2 \times DZ1 \times DA1 \times DRD \times DZ0 \times DB1 \times \overline{DRD} \times \mathcal{F} \tag{24}$$

where DZ1 is given by equation (6) and $\overline{DRD}$ is given by equation (18)

ii) $L_1 + L_2 > L$ and $L_1 \geqslant L_2$ and $L_2 < L$

$$F_2 = DZ1 \times DA1 \times DRD \times DZ0 \times DB1 \times \overline{DRD} \times \mathcal{F} \tag{25}$$

where DZ1 is given by equation (14) and $\overline{DRD}$ by equation (18).

iii) $L_1 + L_2 > L$ and $L_2 > L_1$ and $L_1 < L$

$$F_3 = DZ2 \times DA2 \times DZ1 \times DA1 \times DRD \times \overline{DRD} \times \mathcal{F} \tag{26}$$

where DZ1 is given by equation (6) and $\overline{DRD}$ by equation (20).

iv) $MiN(L_1, L_2) > L$

$$F_4 = DZ1 \times DA1 \times DRD \times \overline{DRD} \times \mathcal{F} \tag{27}$$

where DZ1 is given by equation (14) and $\overline{DRD}$ by equation (20).

Equations (24) through (27) are pole-free representations of the modal equation in different regions of the complex plane. It is clear that the functions F_1, F_2, F_3, and F_4 are not continuous so that they are referred to as the pole-free discontinuous version of the modal equation. It is not surprising that a discontinuous set of functions used to represent the modal equation in different regions of the complex plane can lead to difficulties when used in conjunction with the RFM which requires phase continuity in order to trace lines of constant phase. By examining the asymptotic behavior of the modified Hankel functions of order one-third, it can be shown (see appendix) that within the significant region of the complex plane a continuous representation of the pole-free modal equation is as given below.

Pole-Free Continuous Version of the Modal Equation

i) $L_1 + L_2 < L$

$$M_1 = -\frac{1}{2\beta^3}\left(\frac{\alpha_3}{|\alpha_2|}\right)^{1/6} \exp\left[-\frac{2}{3}i\left\{(p_1(3))^{3/2} + (p_2(2))^{3/2} + (p_1(1))^{3/2}\right\} + \frac{5}{12}\pi i\right] \times F_1 \tag{28}$$

ii) $L_1 + L_2 > L$ and $L_1 \geq L_2$ and $L_2 < L$

$$M_2 = \frac{1}{\beta}\exp\left[-\frac{2}{3}i\,(p_1(1))^{3/2} + \frac{5}{12}\pi i\right] \times F_2 \tag{29}$$

iii) $L_1 + L_2 > L$ and $L_2 > L_1$ and $L_1 < L$

$$M_3 = -\frac{1}{2\beta^2}\left(\frac{\alpha_3}{|\alpha_2|}\right)^{1/6} \frac{DZ0 - NZ0\ \ (s^2 - \alpha_1 D)^{1/2}}{(p_1(1))^{1/4}} \exp\left[-\frac{2}{3}i\left\{(p_2(2))^{3/2} + (p_1(3))^{3/2}\right\}\right] \times F_3 \tag{30}$$

iv) $MIN(L_1, L_2) > L$

$$M_4 = \frac{DZ0 - NZ0\ \ (s^2 - \alpha_1 D)^{1/2}}{(p_1(1))^{1/4}} \times F_4 \tag{31}$$

Equations (28) through (31) describe a pole-free continuous version of the modal equation which will be discussed further in section 6. The continuity factors introduced in equations (28) through (31) introduce branch points along the real axis. The branch points in the denominators of equations (30) and (31) are sinks of phase contours; however, no complications occur as these equations are employed in regions well removed from the branch points. The branch points in the exponential terms of equations (28) through (30) can cause problems due to phase discontinuities across their associated branch cuts. However, it has been found that these discontinuities are not large enough (in the region enclosed by reasonable search rectangles) to interfere with the phase contour tracing of the RFM if the branch cuts are in the lower half of the complex θ plane and sufficiently divergent from the real axis.

6. RESULTS

A previous[5] case study of a ground-based duct produced by an elevated layer (see fig 8) between 183m (600 ft) and 305m (1000 ft) characterized by about a 40m unit deficit (DELM) is reexamined in this section by use of the RFM. As shown in figure 8 the layer height is z_1 and the layer structure is approximated by a trilinear model. The abscissa is the modified refractivity, M ($M = (n-1) \times 10^6$ where n is the modified refractive index), and the ordinate is altitude in metres. The frequencies 65 MHz, 170 MHz, 520 MHz, and 3.3 GHz used in the previous study are reexamined so that a direct comparison of computer run times can be made. The mode attenuation cutoff was 0.5 dB/km for the three lowest frequencies and 1 dB/km for 3.3 GHz. As a result the number of modes used ranged from 2 at 65 MHz to 81 at 3.3 GHz.

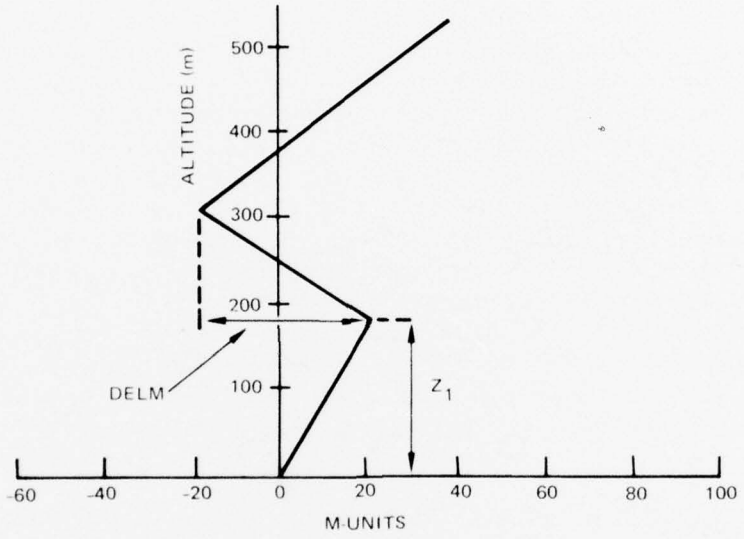

Figure 8. Trilinear modified refractivity profile referenced to zero at the ground.

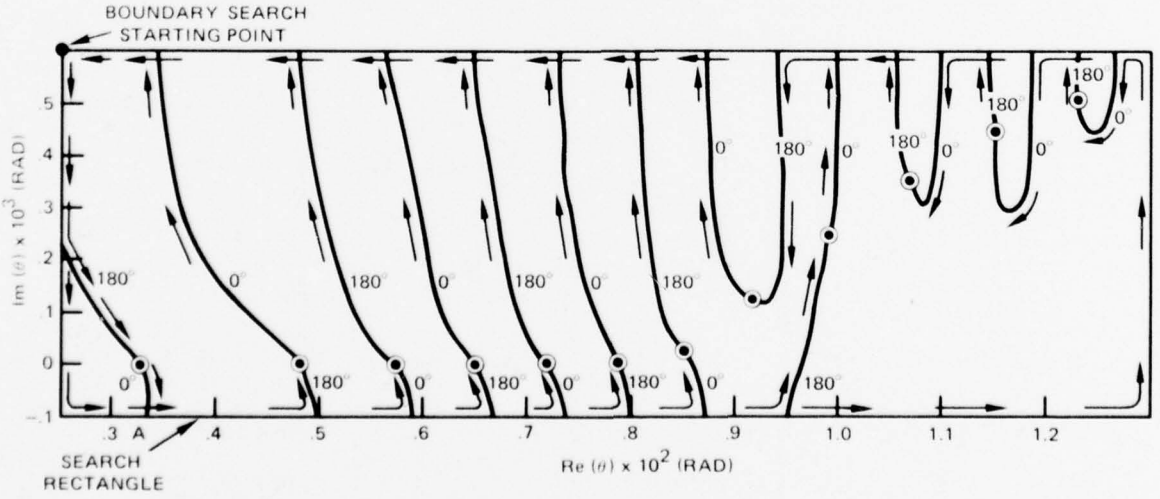

Figure 9. Application of the RFM to the 520 MHz case.
- 0° and 180° phase contours
- Zeros
- Direction of search path

By use of the RFM and the pole-free modal function F_1 defined by equation (24) of section 5 the eigenangles for the three lowest frequencies were obtained without complication, due to the lack of function switching (dealt with in section 5) at these relatively low frequencies (ie, only the function F_1 was used). Figure 9 is a representation of the RFM applied to the 520 MHz case, this being an interesting representative of this lower frequency domain. The ordinate is $\mathrm{Im}(\theta)$ and the abscissa is $\mathrm{Re}(\theta)$. The axes are scaled differently in order to present a clear and complete view of the essential phase contour behavior of the modal function, F_1, in the entire region of the search rectangle. Twelve zeros (or modal solutions) are indicated in the region of theta space shown. These modal solutions are presented in table 1. Since a general description of the RFM has been given previously (section 4), only certain interesting aspects of figure 9 will be singled out. The rectangle boundary search begins at the upper left corner of the search rectangle and proceeds as indicated by the arrows. In the diagram A depicts an example of a point where the tracing of a phase contour stops, having encountered the search rectangle boundary. This location is flagged so as to avoid the retracing of that phase contour at a later time during the boundary search. It is interesting to note that the modes are not found in consecutive order. Due to the phase contour configuration, the ninth mode is found before the eighth, which in turn is not located until last. As can be seen from the figure, the actual order in which the modes are found is 1 through 7, 9, 12, 11, 10, 8. Twelve modes, consistent with the previous work (ref 5) have been found; however, unlike the findings of the previous work, which relied on the Newton-Raphson iteration, it is now certain that all modes within the search rectangle have been found.

Phase contours for the original modal equation $\mathfrak{F}(\theta) = 1 - RR$ (equation 3) are shown in figure 10 for a small region of the complex plane for the frequency 3.3 GHz. The abscissa is $\mathrm{Re}(\theta)$ while the ordinate is $\mathrm{Im}(\theta)$. The modal equation contains poles, four of which are indicated in the figure along with six zeros. The zero at the origin is a mode

TABLE 1. MODAL SOLUTIONS FOR THE 520-MHz CASE.

MODE	$\mathrm{Re}(\theta)$-RAD	$\mathrm{Im}(\theta)$-RAD
1	$.324 \times 10^{-2}$	$.261 \times 10^{-11}$
2	$.480 \times 10^{-2}$	$.370 \times 10^{-9}$
3	$.574 \times 10^{-2}$	$.581 \times 10^{-8}$
4	$.648 \times 10^{-2}$	$.230 \times 10^{-7}$
5	$.719 \times 10^{-2}$	$.844 \times 10^{-7}$
6	$.789 \times 10^{-2}$	$.181 \times 10^{-5}$
7	$.853 \times 10^{-2}$	$.266 \times 10^{-4}$
8	$.918 \times 10^{-2}$	$.123 \times 10^{-3}$
9	$.990 \times 10^{-2}$	$.249 \times 10^{-3}$
10	$.107 \times 10^{-1}$	$.355 \times 10^{-3}$
11	$.115 \times 10^{-1}$	$.451 \times 10^{-3}$
12	$.123 \times 10^{-1}$	$.512 \times 10^{-3}$

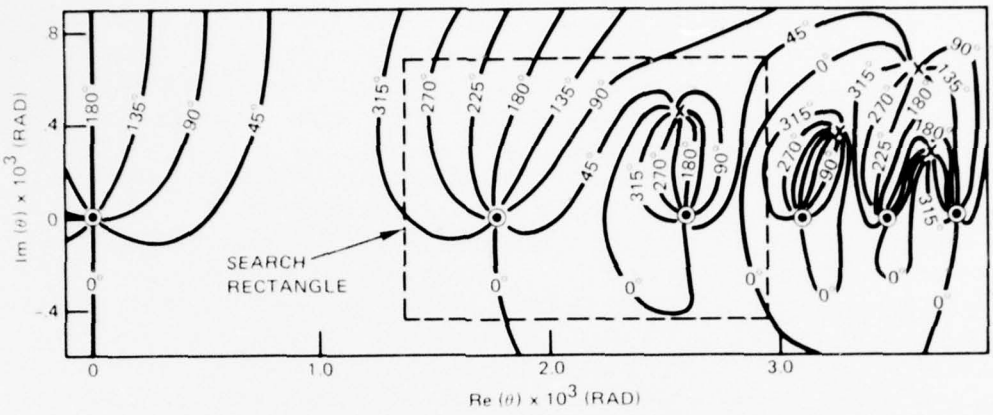

Figure 10. Phase contours for the original modal equation.
◉ Zeros
× Poles

which has zero excitation, therefore it is of no concern. The effect of the poles on the phase contours is clearly evident in the complicated phase contour structure. "Phase line extinction" and its disastrous results can be seen for the hypothetical search rectangle shown (dashed line). The problem is that not all the phase contours associated with the zero at $\mathrm{Re}(\theta) \cong 2.6 \times 10^{-3}$ rad, cross the search rectangle boundary — some are confined to a limited region in the neighborhood of the paired pole and zero. As can be seen, the 0° and 180° phase contours of that zero never cross the search rectangle boundary, therefore the zero would not be located by the RFM. This, then, clearly illustrates the necessity of a pole-free modal equation, at least within the interior of the search rectangle, to assure no missed modal solutions.

Figure 11 shows phase contours, in the same region of the complex plane as figure 10, for the modified modal equation which is pole-free and continuous as discussed in section 5 (see in particular equation (31) and the associated discussion). In contrast to the case for the original modal equation (fig 10) the absence of poles results in a much more relaxed and simplified phase contour behavior. For such a situation the 0° and 180° phase contours

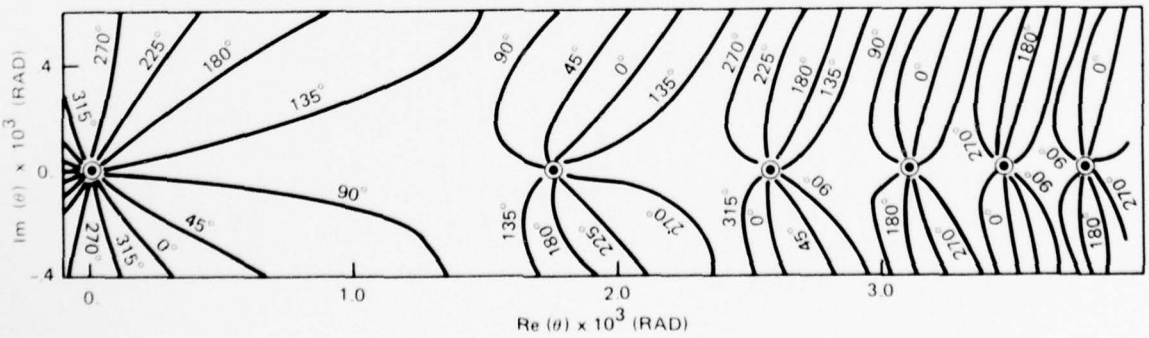

Figure 11. Phase contours for the pole-free continuous version of the modal equation at 3.3 GHz.
◉ Zeros

associated with every zero enclosed by any imaginable search rectangle would cross the boundary of that search rectangle. Therefore, no difficulties would be anticipated when employing the RFM to find mode solutions for this case. It may be noted in figure 11 that the 4π phase change about the zero at the origin is indicative of a second order zero, which resulted from the introduction of a second zero at the origin by the continuity factor in equation 31 (NZ0 = DZ0 = 0 at the origin).

Figure 12 shows phase contours for the same case as figure 11 except the region shown is one of higher order modes (larger θ_I values), where equation (28) of section 5 is used. Only two of the higher order modes are shown. It is seen that spurious phase contours enter and exit the region leading to no mode solutions. As will be pointed out in the next paragraph the source of the spurious contours is the set of continuity factors used to make the pole-free discontinuous version of the modal equation continuous over the full dynamic range in theta space. It is apparent that computer time was spent needlessly tracing many 0° and 180° spurious phase lines. In addition the bending and compacting of the phase lines associated with the two modes is also due to the entrance of the spurious phase contours. The increased density of phase contours required a reduced mesh size which increased the run time even more significantly. The requirement of a small mesh size is clearly illustrated by the two dashed squares which are two hypothetical mesh squares representative of the mesh size that was expected for the mode spacing in the 3.3-GHz case. Mesh square A encloses the 0° and 180° contours of the mode at $\mathrm{Re}(\theta) \cong 11.87 \times 10^{-3}$ radians. The mathematical consequence would be that neither the 0° or 180° contours would be recognized as passing through the mesh square, and the mode would not be located. Mesh square B contains the passage of both a 0° and 90° phase contour. Mathematically it would appear that a mode solution was nearby, leading to a fruitless search for a phantom mode. A smaller mesh size obviously solves these problems due to the higher resolution it offers.

The continuity factors introduced in section 5 and derived in the appendix involve complex exponential terms and as pointed out above are responsible for the spurious phase contours shown in figure 12. Figure 13(a) is an enlarged view of a small region, near the mode at $\mathrm{Re}(\theta) \cong 11.74 \times 10^{-3}$ radians, in figure 12. The remarkable similarity of this diagram with figure 14(c) (which is a composite of figure 14(a) and (b)) clearly illustrates how the type of phase contour behavior seen in figures 12 and 13(a) can result from the presence of a complex exponential factor. The verification that the continuity factors are

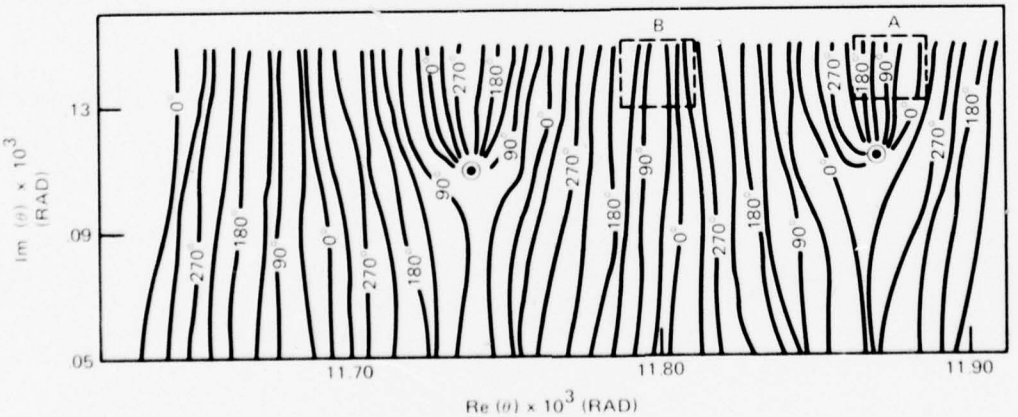

Figure 12. Phase contours in a region of higher-order modes for the pole-free continuous version of the modal equation at 3.3 GHz.

◉ Zeros

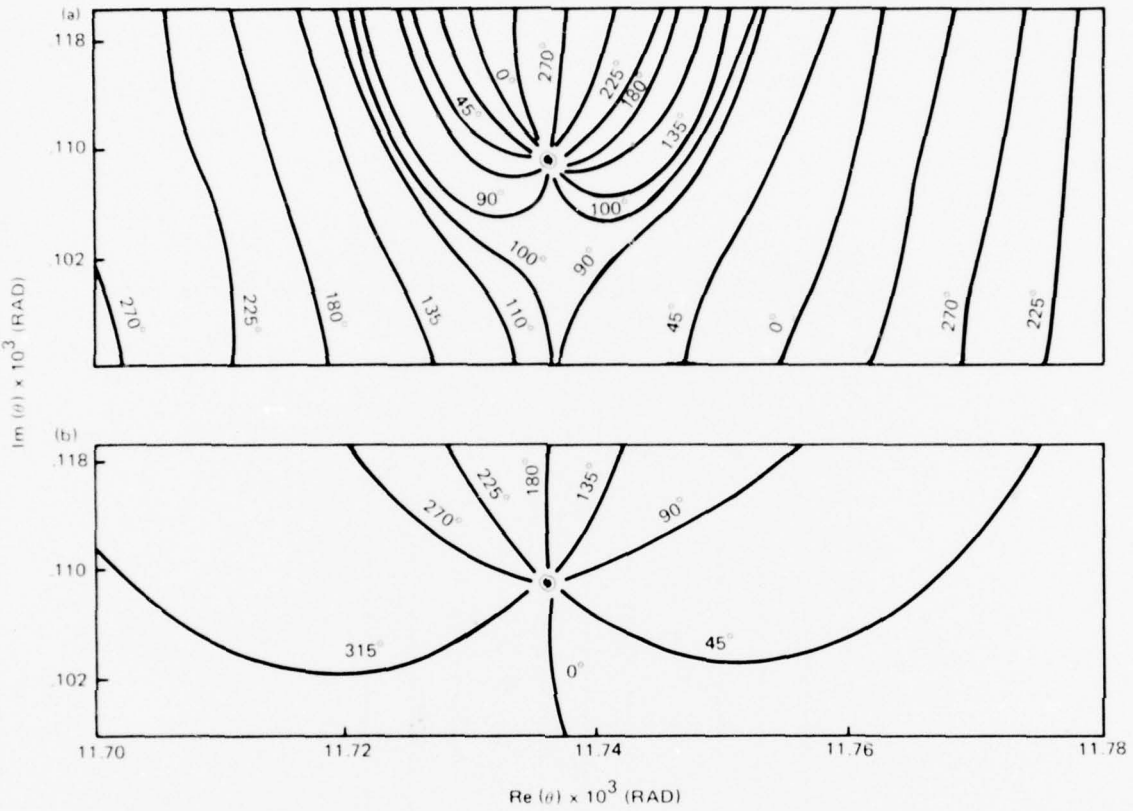

Figure 13. Phase contours in the region of a higher-order mode for two versions of the modal equation at 3.3 GHz.

◉ Zero

(a) Pole-free continuous version of the modal equation

(b) Pole-free discontinuous version of the modal equation

responsible for the spurious phase contour behavior is illustrated by figure 13. Figure 13(a) shows phase contours, in the region of a single mode, for the pole-free continuous modal equation (equation (28) of section 5). Figure 13(b) shows phase contours in the same region for the pole-free discontinuous modal equation (equation (24) of section 5). As can be seen, the absence of the continuity factors in the discontinuous version removes the presence of the spurious phase lines. The resulting simplified phase contour structure allows a significant reduction in computer run time.

The temptation to simply use the discontinuous version must be approached with caution. Figure 15 illustrates a danger of using discontinuous function with the RFM. The same regions of the complex plane are shown in (a) and (b) of the figure. In particular, phase contours of F_1 (equation (24) of section 5) and F_2 (equation (25) of section 5) are plotted in figure 15(a) and figure 15(b), respectively. Each function is used in a separate region of the complex plane. The dashed line denotes a switch boundary. F_1 is used in the region to the right of the switch boundary and F_2 in the region to the left. The type of situation presented in the figure leads to an undetected mode as follows. In the lower left

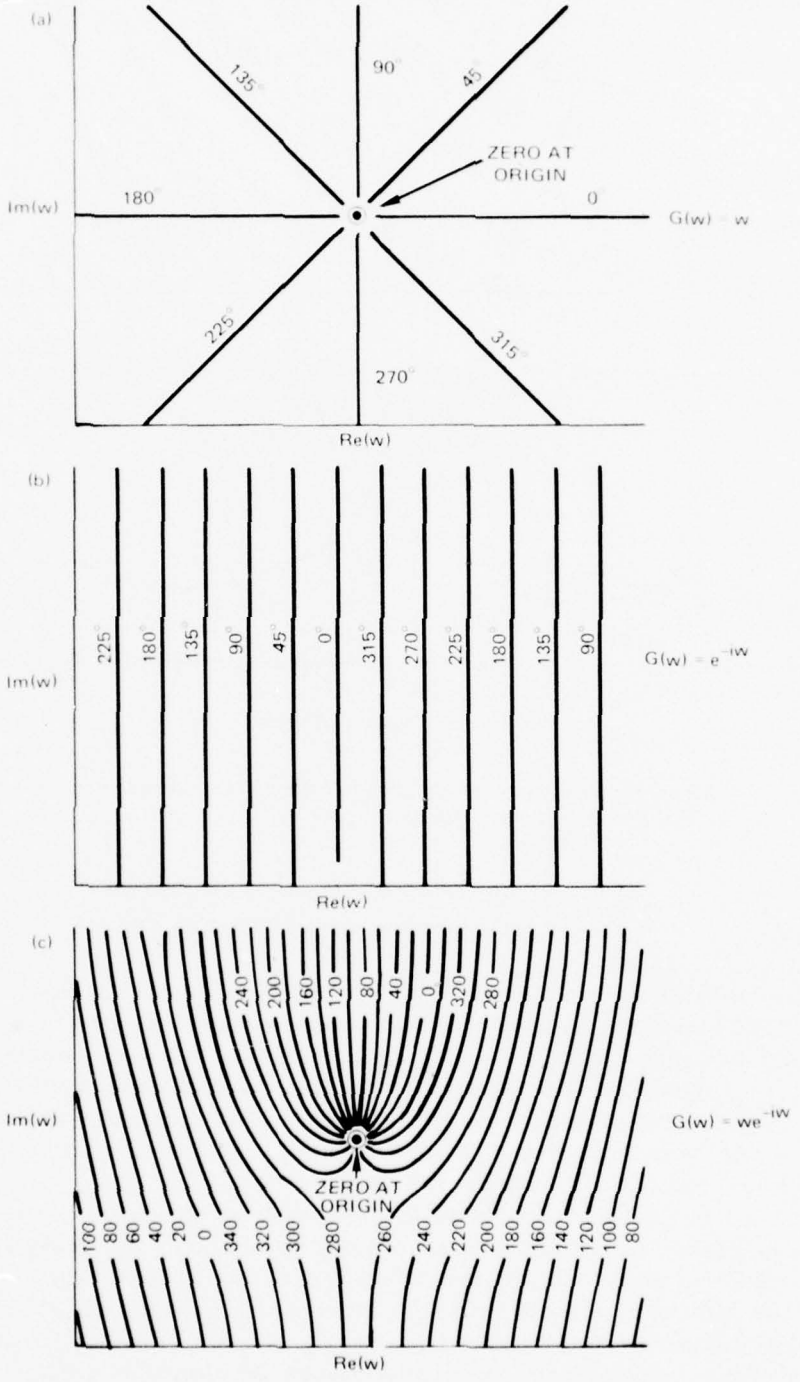

Figure 14. Phase contours for some simple functions.

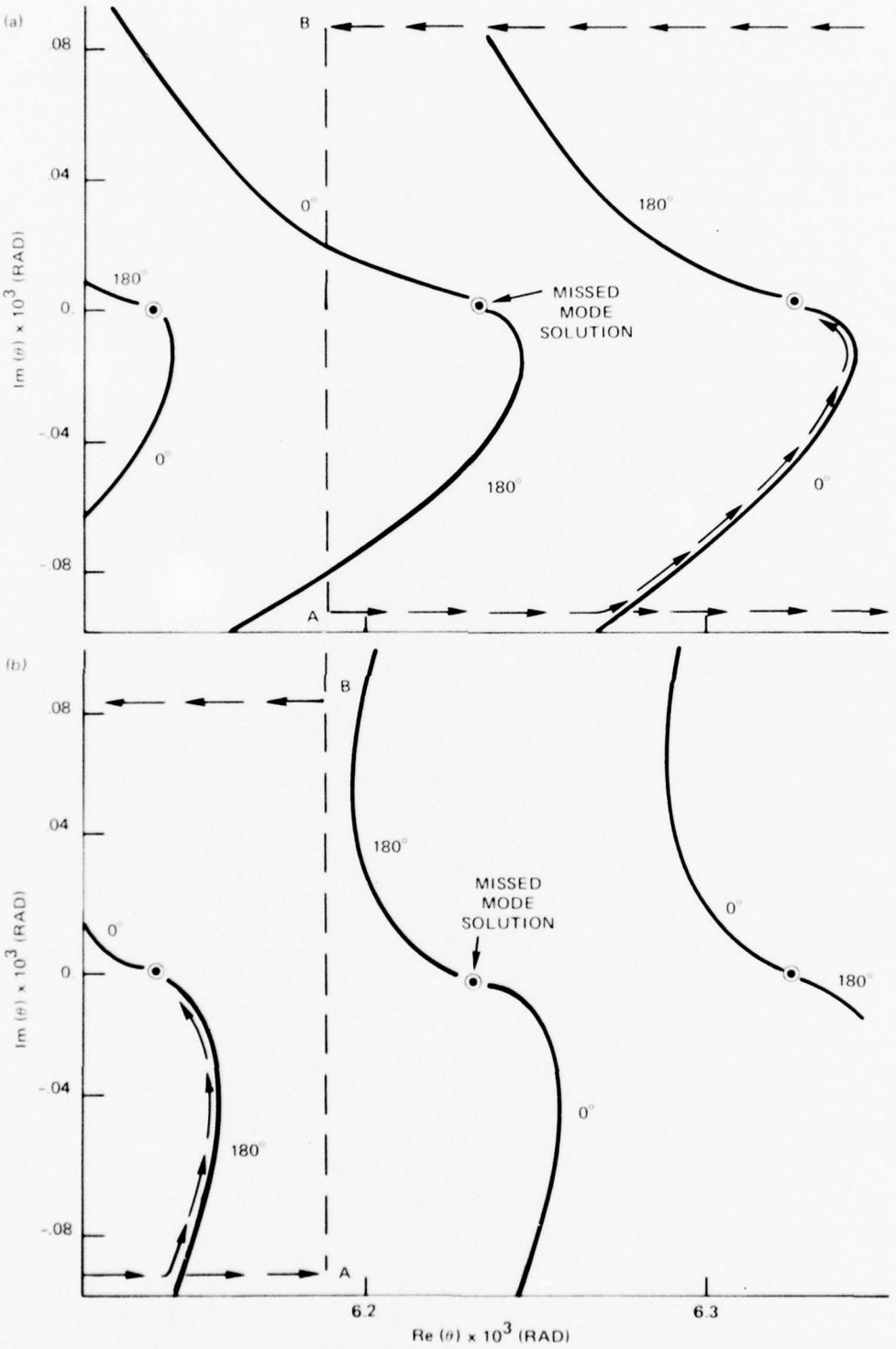

Figure 15. A problem of function switching for the pole-free discontinuous version of the modal equation.

- ◉ Zeros
- ⟶ Direction of search path
- ---- Switch boundary

corner of figure 15(b) it is seen that F_2 would be used in this region during the rectangle boundary search portion of the RFM. The first of the three modes in the diagram would be found via the F_2 180° phase contour associated with it. When the boundary search reached A, the switch to F_1 would be made, and it can be seen that the 0° phase contour of F_2 and the 180° phase contour of F_1 which are associated with the second mode would not be encountered along the search path. Continuing on, the third mode would be located via the 0° phase contour of F_1. When coming back along the top edge of the search rectangle boundary, the switch back to F_2 would be made at B. It is seen that the 0° phase contour of F_1 and the 180° phase contour of F_2 which lead to the second mode would not be encountered. Therefore, the second mode in the diagram would go undetected. This shows, rather clearly, a crucial difficulty encountered in indiscriminately employing the discontinuous version of the modal equation with the RFM.

There is a practical way to use the pole-free discontinuous version of the modal equation. The original search rectangle is divided into two smaller search rectangles at the switch boundary. Now since a single function is used in each rectangular region, the application of the RFM to each separate rectangle will definitely locate all the modes.

Actually for the 3.3 GHz case there were two switch boundaries involved (the other boundary occurred at $\mathrm{Re}(\theta) \cong .47 \times 10^{-3}$ rad). However, instead of dividing the original search rectangle into three smaller search rectangles it was found to be desirable to divide the original search rectangle only at the second switch boundary ($\mathrm{Re}(\theta) \cong 6.2 \times 10^{-3}$ rad) and to use the continuous functions in the region containing the first switch boundary (at $\mathrm{Re}(\theta) \cong 4.7 \times 10^{-3}$ rad). Although the continuous functions, M_4 and M_2 (equations (31) and (29)) are used in the first search rectangle, their associated spurious phase line behavior is not seriously detrimental to the computer run time (actually M_4 contains no spurious phase behavior while M_2 has such behavior but the behavior is less prominent at the lower $\mathrm{Re}(\theta)$ values). This was the procedure actually employed in using the discontinuous version of the modal equation with the RFM.

In general for trilinear profiles of the type depicted in figure 8 there would be four possible switch boundaries and for multisegmented profiles (more than three segments) very likely considerably more than four. It is clear that locating these boundaries for the purpose of search rectangle construction can present a formidable problem. Therefore, the use of discontinuous functions although possible in principle can for general cases be very difficult to implement.

Table 2 lists the computer run times for waveguide runs for the two versions of the RFM along with the previously used Newton-Raphson method. For the 3.3-GHz case the disastrous effect of the spurious phase contours in the continuous version of the modal equation is obvious from the 20-minute run time which is over three times greater than that for the discontinuous version of the modal equation. The Newton-Raphson case was run on an IBM 360 computer while the RFM cases were run on a Univac 1110 computer. A rough

TABLE 2. COMPUTER RUN TIME COMPARISONS.

Freq	Newton-Raphson*	RFM (Pole-Free Continuous)	RFM (Pole-Free Discontinuous)
520 MHz	2 min	2 min	2 min
3.3 GHz	8 min	20 min	6 min

*The Newton method was run on an IBM 360. The presented times are approximate Univac 1110 equivalents.

comparison between the two computers is that the Univac 1110 is twice as fast as the IBM 360. Therefore, the Newton-Raphson run times presented in the table are approximate and were obtained simply by dividing the IBM 360 run time by two. The 520 MHz case has been listed as an example of the lower frequencies. In this domain (as a result of a decrease in the dynamic range requirements) function switching does not occur and spurious phase line behavior is not as prominent. Therefore, only one rectangle is needed for the RFM discontinuous version and extremely small mesh squares are not necessary for the RFM continuous version. The result is equivalent run times for the two methods.

It is clear from the preceding discussion that the RFM is most easily implemented if function switching can altogether be avoided. For this reason a set of tables (tables 3(a) through 3(p)) has been prepared as a guide to the waveguide user. The tables show an estimated maximum frequency, FMAX, below which function switching should not occur for several trilinear layer models and various search rectangles. The method of calculation (based on equation 23 of section 5) should ensure a rather conservative estimate of FMAX (ie, switching should not occur until frequencies somewhat higher than FMAX are encountered).

FMAX is dependent upon profile parameters, search rectangle location, and of course the maximum magnitude allowed by the computer used. All calculations are for a machine capable of handling a maximum number of e^{700} (ie, L = 700 according to the notation of section 5). Values of L other than 700 will be discussed shortly. In all instances the layer gradient α_1 (see fig 1) has been taken as the value for the standard atmosphere, 2.36×10^{-7} m^{-1}. Sixteen tables have been generated, each table being associated with a particular combination of four different layer heights, z_1 (see fig 8) and four different search rectangles (the layer height, z_1, and top right corner, $\mathrm{Re}(\theta)$ and $\mathrm{Im}(\theta)$, of the search rectangle are listed at the head of each table). Four different search rectangles are used. Each search rectangle has a maximum $\mathrm{Re}(\theta)$ value of 1.5×10^{-2} radians while the maximum $\mathrm{Im}(\theta)$ takes on four different values. Each table includes profiles which have various layer strengths or M deficits (DELM) (see fig 8) and various layer gradients α_2 and α_3 (see fig 1). In addition to FMAX the tables give the maximum possible attenuation, ATNU, associated with the search rectangle (ie, the attenuation associated with the upper right corner of the search rectangle).

It was stated that the tables were prepared for a computer that handles a maximum number of e^L where L = 700. For a computer allowing a maximum value of L other than 700, the conversion of FMAX in the tables to the proper value is a simple task as L and FMAX are directly proportional. In other words, if e^{ℓ} is the maximum value allowed by the computer, then the correct maximum frequency, f_ℓ, is obtained by

$$f_\ell = \frac{\ell}{700} \mathrm{FMAX}, \tag{32}$$

where FMAX is the tabulated frequency.

As an example of the use of the tables, we estimate FMAX for the present case study. The profile parameters and search rectangle in the table which are closest to those used in the actual study are: $z_1 = 200$ m, DELM = 40, $\alpha_2 = -.6 \times 10^{-6}$ m^{-1}, $\alpha_3 = .6 \times 10^{-6}$ m^{-1}, $\mathrm{Re}(\theta) = .15 \times 10^{-1}$, and $\mathrm{Im}(\theta) = .15 \times 10^{-3}$ radian. These entries are found in table 3(a), where FMAX is seen to be 1.331×10^{10} Hz. The Univac single precision value for L is 87.5 (ie, let $\ell = 87.5$ in equation (32)), therefore no function switching occurs in the present case for frequencies less than about $(87.5/700) \times 1.331 \times 10^{10}$ Hz $= 1.7 \times 10^9$ Hz.

The tabulated values of FMAX have been obtained by using

$$\text{FMAX} = \frac{L}{\left|\text{Re}\left(\frac{4\pi i}{3c}\,\frac{1}{\alpha_1}\,(s^2 - \alpha_1 z_1)^{3/2}\right)\right| + \left|\text{Re}\left(\frac{4\pi i}{3c}\left(\frac{1}{\alpha_2} + \frac{1}{\alpha_3}\right)\left(s^2 - 2\times 10^{-6}\,\text{DELM}\right)^{3/2}\right)\right|} \tag{33}$$

It should be noted that the value of FMAX is determined by computing the above quantity (equation (33)) at both the upper left and upper right corners of the search rectangle and selecting the smaller of the two values.

TABLE 3(a)

L = 700. $\alpha_1 = .236 \times 10^{-6}\ m^{-1}$

$Re(\theta) = .15 \times 10^{-1}$ Rad $Im(\theta) = .15 \times 10^{-3}$ Rad $Z_1 = 200.$ m

DELM	α_2 (m^{-1})	α_3 (m^{-1})	FMAX (Hz)	ATNU (dB/Km)	DELM	α_2 (m^{-1})	α_3 (m^{-1})	FMAX (Hz)	ATNU (dB/Km)
10.0	-.100-006	.100-006	1.581+010	19.74	20.0	-.100-005	.100-006	1.204+010	15.03
10.0	-.100-006	.236-006	1.889+010	23.58	20.0	-.100-005	.236-006	1.853+010	23.14
10.0	-.100-006	.600-006	2.068+010	25.83	20.0	-.100-005	.600-006	2.442+010	30.49
10.0	-.100-006	.100-005	2.121+010	26.48	20.0	-.100-005	.100-005	2.661+010	33.22
10.0	-.236-006	.100-006	1.889+010	23.58	40.0	-.100-006	.100-006	3.191+009	3.98
10.0	-.236-006	.236-006	2.346+010	29.28	40.0	-.100-006	.236-006	4.329+009	5.41
10.0	-.236-006	.600-006	2.629+010	32.83	40.0	-.100-006	.600-006	5.148+009	6.43
10.0	-.236-006	.100-005	2.714+010	33.89	40.0	-.100-006	.100-005	5.414+009	6.76
10.0	-.600-006	.100-006	2.068+010	25.83	40.0	-.236-006	.100-006	4.329+009	5.41
10.0	-.600-006	.236-006	2.629+010	32.83	40.0	-.236-006	.236-006	6.729+009	8.40
10.0	-.600-006	.600-006	2.991+010	37.34	40.0	-.236-006	.600-006	8.939+009	11.16
10.0	-.600-006	.100-005	3.101+010	38.72	40.0	-.236-006	.100-005	9.772+009	12.20
10.0	-.100-005	.100-006	2.121+010	26.48	40.0	-.600-006	.100-006	5.148+009	6.43
10.0	-.100-005	.236-006	2.714+010	33.89	40.0	-.600-006	.236-006	8.939+009	11.16
10.0	-.100-005	.600-006	3.101+010	38.72	40.0	-.600-006	.600-006	1.331+010	16.62
10.0	-.100-005	.100-005	3.221+010	40.21	40.0	-.600-006	.100-005	1.525+010	19.03
20.0	-.100-006	.100-006	7.776+009	9.71	40.0	-.100-005	.100-006	5.414+009	6.76
20.0	-.100-006	.236-006	1.005+010	12.55	40.0	-.100-005	.236-006	9.772+009	12.20
20.0	-.100-006	.600-006	1.157+010	14.44	40.0	-.100-005	.600-006	1.525+010	19.03
20.0	-.100-006	.100-005	1.204+010	15.03	40.0	-.100-005	.100-005	1.784+010	22.27
20.0	-.236-006	.100-006	1.005+010	12.55					
20.0	-.236-006	.236-006	1.422+010	17.75					
20.0	-.236-006	.600-006	1.745+010	21.78					
20.0	-.236-006	.100-005	1.853+010	23.14					
20.0	-.600-006	.100-006	1.157+010	14.44					
20.0	-.600-006	.236-006	1.745+010	21.78					
20.0	-.600-006	.600-006	2.256+010	28.17					
20.0	-.600-006	.100-005	2.442+010	30.49					

TABLE 3(b)

$L = 700.$ $\alpha_1 = .236 \times 10^{-6}\ m^{-1}$

$Re(\theta) = .15 \times 10^{-1}$ Rad $Im(\theta) = .50 \times 10^{-3}$ Rad $Z_1 = 200.$ m

DELM	$\alpha_2 (m^{-1})$	$\alpha_3 (m^{-1})$	FMAX (Hz)	ATNU (dB/km)	DELM	$\alpha_2 (m^{-1})$	$\alpha_3 (m^{-1})$	FMAX (Hz)	ATNU (dB/km)
10.0	-.100-006	.100-006	6.496+009	27.04	20.0	-.100-005	.100-006	1.081+010	44.98
10.0	-.100-006	.236-006	8.556+009	35.61	20.0	-.100-005	.236-006	1.744+010	72.59
10.0	-.100-006	.600-006	9.965+009	41.47	20.0	-.100-005	.600-006	2.402+010	99.97
10.0	-.100-006	.100-005	1.041+010	43.32	20.0	-.100-005	.100-005	2.641+010	109.90
10.0	-.236-006	.100-006	8.556+009	35.61	40.0	-.100-006	.100-006	3.177+009	13.22
10.0	-.236-006	.236-006	1.253+010	52.13	40.0	-.100-006	.236-006	4.309+009	17.93
10.0	-.236-006	.600-006	1.580+010	65.74	40.0	-.100-006	.600-006	5.124+009	21.33
10.0	-.236-006	.100-005	1.694+010	70.52	40.0	-.100-006	.100-005	5.388+009	22.42
10.0	-.600-006	.100-006	9.965+009	41.47	40.0	-.236-006	.100-006	4.309+009	17.93
10.0	-.600-006	.236-006	1.580+010	65.74	40.0	-.236-006	.236-006	6.697+009	27.87
10.0	-.600-006	.600-006	2.138+010	88.97	40.0	-.236-006	.600-006	8.895+009	37.02
10.0	-.600-006	.100-005	2.354+010	97.95	40.0	-.236-006	.100-005	9.722+009	40.46
10.0	-.100-005	.100-006	1.041+010	43.32	40.0	-.600-006	.100-006	5.124+009	21.33
10.0	-.100-005	.236-006	1.694+010	70.52	40.0	-.600-006	.236-006	8.895+009	37.02
10.0	-.100-005	.600-006	2.354+010	97.95	40.0	-.600-006	.600-006	1.324+010	55.11
10.0	-.100-005	.100-005	2.618+010	108.94	40.0	-.600-006	.100-005	1.516+010	63.10
20.0	-.100-006	.100-006	6.780+009	28.22	40.0	-.100-005	.100-006	5.388+009	22.42
20.0	-.100-006	.236-006	8.905+009	37.06	40.0	-.100-005	.236-006	9.722+009	40.46
20.0	-.100-006	.600-006	1.035+010	43.08	40.0	-.100-005	.600-006	1.516+010	63.10
20.0	-.100-006	.100-005	1.081+010	44.98	40.0	-.100-005	.100-005	1.774+010	73.81
20.0	-.236-006	.100-006	8.905+009	37.06					
20.0	-.236-006	.236-006	1.297+010	53.98					
20.0	-.236-006	.600-006	1.629+010	67.78					
20.0	-.236-006	.100-005	1.744+010	72.59					
20.0	-.600-006	.100-006	1.035+010	43.08					
20.0	-.600-006	.236-006	1.629+010	67.78					
20.0	-.600-006	.600-006	2.188+010	91.06					
20.0	-.600-006	.100-005	2.402+010	99.97					

TABLE 3(c)

$L = 700.$ $\alpha_1 = .236 \times 10^{-6}\ m^{-1}$

$Re(\theta) = .15 \times 10^{-1}$ Rad $Im(\theta) = .15 \times 10^{-2}$ Rad $Z_1 = 200.$ m

DELM	γ_2 (m^{-1})	γ_3 (m^{-1})	FMAX (Hz)	ATNU (dB/km)	DELM	γ_2 (m^{-1})	γ_3 (m^{-1})	FMAX (Hz)	ATNU (dB/km)
10.0	-.100-006	.100-006	2.172+009	27.12	20.0	-.100-005	.100-006	3.614+009	45.12
10.0	-.100-006	.236-006	2.861+009	35.72	20.0	-.100-005	.236-006	5.833+009	72.83
10.0	-.100-006	.600-006	3.332+009	41.60	20.0	-.100-005	.600-006	8.033+009	100.29
10.0	-.100-006	.100-005	3.481+009	43.46	20.0	-.100-005	.100-005	8.904+009	111.17
10.0	-.236-006	.100-006	2.861+009	35.72	40.0	-.100-006	.100-006	2.506+009	31.28
10.0	-.236-006	.236-006	4.189+009	52.30	40.0	-.100-006	.236-006	3.268+009	40.81
10.0	-.236-006	.600-006	5.282+009	65.95	40.0	-.100-006	.600-006	3.782+009	47.22
10.0	-.236-006	.100-005	5.666+009	70.74	40.0	-.100-006	.100-005	3.943+009	49.23
10.0	-.600-006	.100-006	3.332+009	41.60	40.0	-.236-006	.100-006	3.268+009	40.81
10.0	-.600-006	.236-006	5.282+009	65.95	40.0	-.236-006	.236-006	4.700+009	58.67
10.0	-.600-006	.600-006	7.149+009	89.26	40.0	-.236-006	.600-006	5.840+009	72.91
10.0	-.600-006	.100-005	7.870+009	98.26	40.0	-.236-006	.100-005	6.232+009	77.81
10.0	-.100-005	.100-006	3.481+009	43.46	40.0	-.600-006	.100-006	3.782+009	47.22
10.0	-.100-005	.236-006	5.666+009	70.74	40.0	-.600-006	.236-006	5.840+009	72.91
10.0	-.100-005	.600-006	7.870+009	98.26	40.0	-.600-006	.600-006	7.712+009	96.28
10.0	-.100-005	.100-005	8.754+009	109.29	40.0	-.600-006	.100-005	8.411+009	105.01
20.0	-.100-006	.100-006	2.267+009	28.31	40.0	-.100-005	.100-006	3.943+009	49.23
20.0	-.100-006	.236-006	2.978+009	37.18	40.0	-.100-005	.236-006	6.232+009	77.81
20.0	-.100-006	.600-006	3.462+009	43.22	40.0	-.100-005	.600-006	8.411+009	105.01
20.0	-.100-006	.100-005	3.614+009	45.12	40.0	-.100-005	.100-005	9.249+009	115.48
20.0	-.236-006	.100-006	2.978+009	37.18					
20.0	-.236-006	.236-006	4.337+009	54.15					
20.0	-.236-006	.600-006	5.446+009	68.00					
20.0	-.236-006	.100-005	5.833+009	72.83					
20.0	-.600-006	.100-006	3.462+009	43.22					
20.0	-.600-006	.236-006	5.446+009	68.00					
20.0	-.600-006	.600-006	7.317+009	91.36					
20.0	-.600-006	.100-005	8.033+009	100.29					

TABLE 3(d)

$L = 700.$ $\alpha_1 = .236 \times 10^{-6}\ m^{-1}$

$Re(\theta) = .15 \times 10^{-1}$ Rad $Im(\theta) = .50 \times 10^{-2}$ Rad $Z_1 = 200.\ m$

DELM	$\alpha_2\ (m^{-1})$	$\alpha_3\ (m^{-1})$	FMAX (HZ)	ATNU (dB/km)	DELM	$\alpha_2\ (m^{-1})$	$\alpha_3\ (m^{-1})$	FMAX (HZ)	ATNU (dB/km)
10.0	-.100-006	.100-006	6.757+008	28.12	20.0	-.100-005	.100-006	1.126+009	46.85
10.0	-.100-006	.236-006	8.901+008	37.04	20.0	-.100-005	.236-006	1.817+009	75.62
10.0	-.100-006	.600-006	1.037+009	43.15	20.0	-.100-005	.600-006	2.503+009	104.15
10.0	-.100-006	.100-005	1.083+009	45.07	20.0	-.100-005	.100-005	2.774+009	115.45
10.0	-.236-006	.100-006	8.901+008	37.04	40.0	-.100-006	.100-006	7.818+008	32.54
10.0	-.236-006	.236-006	1.303+009	54.25	40.0	-.100-006	.236-006	1.020+009	42.44
10.0	-.236-006	.600-006	1.644+009	68.42	40.0	-.100-006	.600-006	1.180+009	49.11
10.0	-.236-006	.100-005	1.764+009	73.39	40.0	-.100-006	.100-005	1.230+009	51.19
10.0	-.600-006	.100-006	1.037+009	43.15	40.0	-.236-006	.100-006	1.020+009	42.44
10.0	-.600-006	.236-006	1.644+009	68.42	40.0	-.236-006	.236-006	1.466+009	61.01
10.0	-.600-006	.600-006	2.226+009	92.63	40.0	-.236-006	.600-006	1.821+009	75.81
10.0	-.600-006	.100-005	2.450+009	101.98	40.0	-.236-006	.100-005	1.944+009	80.89
10.0	-.100-005	.100-006	1.083+009	45.07	40.0	-.600-006	.100-006	1.180+009	49.11
10.0	-.100-005	.236-006	1.764+009	73.39	40.0	-.600-006	.236-006	1.821+009	75.81
10.0	-.100-005	.600-006	2.450+009	101.98	40.0	-.600-006	.600-006	2.405+009	100.08
10.0	-.100-005	.100-005	2.726+009	113.44	40.0	-.600-006	.100-005	2.622+009	109.14
20.0	-.100-006	.100-006	7.062+008	29.39	40.0	-.100-005	.100-006	1.230+009	51.19
20.0	-.100-006	.236-006	9.276+008	38.60	40.0	-.100-005	.236-006	1.944+009	80.89
20.0	-.100-006	.600-006	1.078+009	44.88	40.0	-.100-005	.600-006	2.622+009	109.14
20.0	-.100-006	.100-005	1.126+009	46.85	40.0	-.100-005	.100-005	2.884+009	120.01
20.0	-.236-006	.100-006	9.276+008	38.60					
20.0	-.236-006	.236-006	1.351+009	56.23					
20.0	-.236-006	.600-006	1.697+009	70.61					
20.0	-.236-006	.100-005	1.817+009	75.62					
20.0	-.600-006	.100-006	1.078+009	44.88					
20.0	-.600-006	.236-006	1.697+009	70.61					
20.0	-.600-006	.600-006	2.280+009	94.87					
20.0	-.600-006	.100-005	2.503+009	104.15					

TABLE 3 (e)

$L = 700.$ $\alpha_1 = .236 \times 10^{-6}\ m^{-1}$

$Re(\theta) = .15 \times 10^{-1}$ Rad $Im(\theta) = .15 \times 10^{-3}$ Rad $Z_1 = 500.$ m

DELM	α_2 (m^{-1})	α_3 (m^{-1})	FMAX (Hz)	ATNU (dB/km)	DELM	α_2 (m^{-1})	α_3 (m^{-1})	FMAX (Hz)	ATNU (dB/km)
10.0	-.100-006	.100-006	6.929+009	8.65	20.0	-.100-005	.100-006	6.092+009	7.61
10.0	-.100-006	.236-006	7.462+009	9.32	20.0	-.100-005	.236-006	7.406+009	9.25
10.0	-.100-006	.600-006	7.727+009	9.65	20.0	-.100-005	.600-006	8.195+009	10.23
10.0	-.100-006	.100-005	7.799+009	9.74	20.0	-.100-005	.100-005	8.428+009	10.52
10.0	-.236-006	.100-006	7.462+009	9.32	40.0	-.100-006	.100-006	2.535+009	3.17
10.0	-.236-006	.236-006	8.004+009	10.09	40.0	-.100-006	.236-006	3.204+009	4.00
10.0	-.236-006	.600-006	8.396+009	10.48	40.0	-.100-006	.600-006	3.632+009	4.53
10.0	-.236-006	.100-005	8.481+009	10.59	40.0	-.100-006	.100-005	3.762+009	4.70
10.0	-.600-006	.100-006	7.727+009	9.65	40.0	-.236-006	.100-006	3.204+009	4.00
10.0	-.600-006	.236-006	8.396+009	10.48	40.0	-.236-006	.236-006	4.354+009	5.44
10.0	-.600-006	.600-006	8.733+009	10.90	40.0	-.236-006	.600-006	5.183+009	6.47
10.0	-.600-006	.100-005	8.825+009	11.02	40.0	-.236-006	.100-005	5.452+009	6.81
10.0	-.100-005	.100-006	7.799+009	9.74	40.0	-.600-006	.100-006	3.632+009	4.53
10.0	-.100-005	.236-006	8.481+009	10.59	40.0	-.600-006	.236-006	5.183+009	6.47
10.0	-.100-005	.600-006	8.825+009	11.02	40.0	-.600-006	.600-006	6.402+009	7.99
10.0	-.100-005	.100-005	8.919+009	11.14	40.0	-.600-006	.100-005	6.818+009	8.51
20.0	-.100-006	.100-006	4.769+009	5.95	40.0	-.100-005	.100-006	3.762+009	4.70
20.0	-.100-006	.236-006	5.539+009	6.92	40.0	-.100-005	.236-006	5.452+009	6.81
20.0	-.100-006	.600-006	5.969+009	7.45	40.0	-.100-005	.600-006	6.818+009	8.51
20.0	-.100-006	.100-005	6.092+009	7.61	40.0	-.100-005	.100-005	7.292+009	9.10
20.0	-.236-006	.100-006	5.539+009	6.92					
20.0	-.236-006	.236-006	6.605+009	8.25					
20.0	-.236-006	.600-006	7.226+009	9.02					
20.0	-.236-006	.100-005	7.406+009	9.25					
20.0	-.600-006	.100-006	5.969+009	7.45					
20.0	-.600-006	.236-006	7.226+009	9.02					
20.0	-.600-006	.600-006	7.975+009	9.96					
20.0	-.600-006	.100-005	8.195+009	10.23					

TABLE 3(f)

L = 700. $\alpha_1 = .236 \times 10^{-6}$ m^{-1}

Re(θ) = $.15 \times 10^{-1}$ Rad Im(θ) = $.50 \times 10^{-3}$ Rad Z_1 = 500. m

DELM	γ_2 (m^{-1})	γ_3 (m^{-1})	FMAX (Hz)	ATNU (dB/km)	DELM	γ_2 (m^{-1})	γ_3 (m^{-1})	FMAX (Hz)	ATNU (dB/km)
10.0	-.100-006	.100-006	6.746+009	28.07	20.0	-.100-005	.100-006	6.062+009	25.23
10.0	-.100-006	.236-006	7.420+009	30.88	20.0	-.100-005	.236-006	7.377+009	30.70
10.0	-.100-006	.600-006	7.687+009	31.99	20.0	-.100-005	.600-006	8.166+009	33.99
10.0	-.100-006	.100-005	7.759+009	32.29	20.0	-.100-005	.100-005	8.399+009	34.96
10.0	-.236-006	.100-006	7.420+009	30.88	40.0	-.100-006	.100-006	2.525+009	10.51
10.0	-.236-006	.236-006	8.046+009	33.49	40.0	-.100-006	.236-006	3.192+009	13.29
10.0	-.236-006	.600-006	8.361+009	34.80	40.0	-.100-006	.600-006	3.619+009	15.06
10.0	-.236-006	.100-005	8.447+009	35.15	40.0	-.100-006	.100-005	3.749+009	15.60
10.0	-.600-006	.100-006	7.687+009	31.99	40.0	-.236-006	.100-006	3.192+009	13.29
10.0	-.600-006	.236-006	8.361+009	34.80	40.0	-.236-006	.236-006	4.338+009	18.05
10.0	-.600-006	.600-006	8.701+009	36.21	40.0	-.236-006	.600-006	5.165+009	21.49
10.0	-.600-006	.100-005	8.794+009	36.60	40.0	-.236-006	.100-005	5.433+009	22.61
10.0	-.100-005	.100-006	7.759+009	32.29	40.0	-.600-006	.100-006	3.619+009	15.06
10.0	-.100-005	.236-006	8.447+009	35.15	40.0	-.600-006	.236-006	5.165+009	21.49
10.0	-.100-005	.600-006	8.794+009	36.60	40.0	-.600-006	.600-006	6.381+009	26.56
10.0	-.100-005	.100-005	8.889+009	36.99	40.0	-.600-006	.100-005	6.796+009	28.28
20.0	-.100-006	.100-006	4.743+009	19.74	40.0	-.100-005	.100-006	3.749+009	15.60
20.0	-.100-006	.236-006	5.511+009	22.93	40.0	-.100-005	.236-006	5.433+009	22.61
20.0	-.100-006	.600-006	5.940+009	24.72	40.0	-.100-005	.600-006	6.796+009	28.28
20.0	-.100-006	.100-005	6.062+009	25.23	40.0	-.100-005	.100-005	7.269+009	30.25
20.0	-.236-006	.100-006	5.511+009	22.93					
20.0	-.236-006	.236-006	6.576+009	27.37					
20.0	-.236-006	.600-006	7.196+009	29.95					
20.0	-.236-006	.100-005	7.377+009	30.70					
20.0	-.600-006	.100-006	5.940+009	24.72					
20.0	-.600-006	.236-006	7.196+009	29.95					
20.0	-.600-006	.600-006	7.946+009	33.07					
20.0	-.600-006	.100-005	8.166+009	33.99					

TABLE 3(g)

$L = 700.$ $\alpha_1 = .236 \times 10^{-6}\ m^{-1}$

$Re(\theta) = .15 \times 10^{-1}$ Rad $Im(\theta) = .15 \times 10^{-2}$ Rad $Z_1 = 500.\ m$

DELH	$\alpha_2\ (m^{-1})$	$\alpha_3\ (m^{-1})$	FMAX (Hz)	ATNU (dB/km)	DELH	$\alpha_2\ (m^{-1})$	$\alpha_3\ (m^{-1})$	FMAX (Hz)	ATNU (dB/km)
10.0	-.100-006	.100-006	2.256+009	28.16	20.0	-.100-005	.100-006	3.851+009	48.08
10.0	-.100-006	.236-006	3.007+009	37.54	20.0	-.100-005	.236-006	6.475+009	80.84
10.0	-.100-006	.600-006	3.532+009	44.10	20.0	-.100-005	.600-006	7.921+009	98.89
10.0	-.100-006	.100-005	3.700+009	46.19	20.0	-.100-005	.100-005	8.157+009	101.84
10.0	-.236-006	.100-006	3.007+009	37.54	40.0	-.100-006	.100-006	2.442+009	30.49
10.0	-.236-006	.236-006	4.510+009	56.30	40.0	-.100-006	.236-006	3.089+009	38.57
10.0	-.236-006	.600-006	5.803+009	72.46	40.0	-.100-006	.600-006	3.504+009	43.74
10.0	-.236-006	.100-005	6.270+009	78.28	40.0	-.100-006	.100-005	3.630+009	45.32
10.0	-.600-006	.100-006	3.532+009	44.10	40.0	-.236-006	.100-006	3.089+009	38.57
10.0	-.600-006	.236-006	5.803+009	72.46	40.0	-.236-006	.236-006	4.204+009	52.49
10.0	-.600-006	.600-006	8.138+009	101.60	40.0	-.236-006	.600-006	5.011+009	62.56
10.0	-.600-006	.100-005	8.531+009	106.51	40.0	-.236-006	.100-005	5.273+009	65.83
10.0	-.100-005	.100-006	3.700+009	46.19	40.0	-.600-006	.100-006	3.504+009	43.74
10.0	-.100-005	.236-006	6.270+009	78.28	40.0	-.600-006	.236-006	5.011+009	62.56
10.0	-.100-005	.600-006	8.531+009	106.51	40.0	-.600-006	.600-006	6.200+009	77.41
10.0	-.100-005	.100-005	8.634+009	107.80	40.0	-.600-006	.100-005	6.607+009	82.49
20.0	-.100-006	.100-006	2.358+009	29.44	40.0	-.100-005	.100-006	3.630+009	45.32
20.0	-.100-006	.236-006	3.137+009	39.16	40.0	-.100-005	.236-006	5.273+009	65.83
20.0	-.100-006	.600-006	3.678+009	45.92	40.0	-.100-005	.600-006	6.607+009	82.49
20.0	-.100-006	.100-005	3.851+009	48.08	40.0	-.100-005	.100-005	7.071+009	88.28
20.0	-.236-006	.100-006	3.137+009	39.16					
20.0	-.236-006	.236-006	4.682+009	58.46					
20.0	-.236-006	.600-006	6.002+009	74.93					
20.0	-.236-006	.100-005	6.475+009	80.84					
20.0	-.600-006	.100-006	3.678+009	45.92					
20.0	-.600-006	.236-006	6.002+009	74.93					
20.0	-.600-006	.600-006	7.698+009	96.11					
20.0	-.600-006	.100-005	7.921+009	98.89					

TABLE 3(b)

$L = 700.$ $\alpha_1 = .236 \times 10^{-6}\ m^{-1}$

$Re(\theta) = .15 \times 10^{-1}$ Rad $Im(\theta) = .50 \times 10^{-2}$ Rad $Z_1 = 500.$ m

DELM	$\gamma_2\ (m^{-1})$	$\gamma_3\ (m^{-1})$	FMAX (Hz)	ATNU (dB/km)
10.0	-.100-006	.100-006	7.016+008	29.20
10.0	-.100-006	.236-006	9.354+008	38.93
10.0	-.100-006	.600-006	1.099+009	45.73
10.0	-.100-006	.100-005	1.151+009	47.90
10.0	-.236-006	.100-006	9.354+008	38.93
10.0	-.236-006	.236-006	1.403+009	58.39
10.0	-.236-006	.600-006	1.806+009	75.15
10.0	-.236-006	.100-005	1.951+009	81.20
10.0	-.600-006	.100-006	1.099+009	45.73
10.0	-.600-006	.236-006	1.806+009	75.15
10.0	-.600-006	.600-006	2.533+009	105.41
10.0	-.600-006	.100-005	2.828+009	117.70
10.0	-.100-005	.100-006	1.151+009	47.90
10.0	-.100-005	.236-006	1.951+009	81.20
10.0	-.100-005	.600-006	2.828+009	117.70
10.0	-.100-005	.100-005	3.201+009	133.23
20.0	-.100-006	.100-006	7.345+008	30.57
20.0	-.100-006	.236-006	9.769+008	40.66
20.0	-.100-006	.600-006	1.146+009	47.68
20.0	-.100-006	.100-005	1.199+009	49.91
20.0	-.236-006	.100-006	9.769+008	40.66
20.0	-.236-006	.236-006	1.458+009	60.70
20.0	-.236-006	.600-006	1.869+009	77.80
20.0	-.236-006	.100-005	2.017+009	83.94
20.0	-.600-006	.100-006	1.146+009	47.68
20.0	-.600-006	.236-006	1.869+009	77.80
20.0	-.600-006	.600-006	2.603+009	108.33
20.0	-.600-006	.100-005	2.898+009	120.60
20.0	-.100-005	.100-006	1.199+009	49.91
20.0	-.100-005	.236-006	2.017+009	83.94
20.0	-.100-005	.600-006	2.898+009	120.60
20.0	-.100-005	.100-005	3.268+009	136.01
40.0	-.100-006	.100-006	8.166+008	33.98
40.0	-.100-006	.236-006	1.080+009	44.94
40.0	-.100-006	.600-006	1.261+009	52.48
40.0	-.100-006	.100-005	1.318+009	54.87
40.0	-.236-006	.100-006	1.080+009	44.94
40.0	-.236-006	.236-006	1.593+009	66.31
40.0	-.236-006	.600-006	2.022+009	84.16
40.0	-.236-006	.100-005	2.174+009	90.48
40.0	-.600-006	.100-006	1.261+009	52.48
40.0	-.600-006	.236-006	2.022+009	84.16
40.0	-.600-006	.600-006	2.767+009	115.17
40.0	-.600-006	.100-005	3.060+009	127.34
40.0	-.100-005	.100-006	1.318+009	54.87
40.0	-.100-005	.236-006	2.174+009	90.48
40.0	-.100-005	.600-006	3.060+009	127.34
40.0	-.100-005	.100-005	3.421+009	142.38

TABLE 3(i)

$L = 700.$ $\alpha_1 = .236 \times 10^{-6}\ m^{-1}$

$Re(\theta) = .15 \times 10^{-1}$ Rad $Im(\theta) = .15 \times 10^{-3}$ Rad $Z_1 = 1000.$ m

DELM	$\alpha_2\ (m^{-1})$	$\alpha_3\ (m^{-1})$	FMAX (Hz)	ATNU (dB/km)	DELM	$\alpha_2\ (m^{-1})$	$\alpha_3\ (m^{-1})$	FMAX (Hz)	ATNU (dB/km)
10.0	-.100-006	.100-006	2.918+009	3.64	20.0	-.100-005	.100-006	2.758+009	3.44
10.0	-.100-006	.236-006	3.008+009	3.76	20.0	-.100-005	.236-006	2.999+009	3.74
10.0	-.100-006	.600-006	3.050+009	3.81	20.0	-.100-005	.600-006	3.121+009	3.90
10.0	-.100-006	.100-005	3.061+009	3.82	20.0	-.100-005	.100-005	3.154+009	3.94
10.0	-.236-006	.100-006	3.008+009	3.76	40.0	-.100-006	.100-006	1.687+009	2.11
10.0	-.236-006	.236-006	3.104+009	3.88	40.0	-.100-006	.236-006	1.959+009	2.45
10.0	-.236-006	.600-006	3.149+009	3.93	40.0	-.100-006	.600-006	2.111+009	2.64
10.0	-.236-006	.100-005	3.161+009	3.95	40.0	-.100-006	.100-005	2.154+009	2.69
10.0	-.600-006	.100-006	3.050+009	3.81	40.0	-.236-006	.100-006	1.959+009	2.45
10.0	-.600-006	.236-006	3.149+009	3.93	40.0	-.236-006	.236-006	2.336+009	2.92
10.0	-.600-006	.600-006	3.196+009	3.99	40.0	-.236-006	.600-006	2.555+009	3.19
10.0	-.600-006	.100-005	3.208+009	4.00	40.0	-.236-006	.100-005	2.619+009	3.27
10.0	-.100-005	.100-006	3.061+009	3.82	40.0	-.600-006	.100-006	2.111+009	2.64
10.0	-.100-005	.236-006	3.161+009	3.95	40.0	-.600-006	.236-006	2.555+009	3.19
10.0	-.100-005	.600-006	3.208+009	4.00	40.0	-.600-006	.600-006	2.820+009	3.52
10.0	-.100-005	.100-005	3.220+009	4.02	40.0	-.600-006	.100-005	2.898+009	3.62
20.0	-.100-006	.100-006	2.450+009	3.06	40.0	-.100-005	.100-006	2.154+009	2.69
20.0	-.100-006	.236-006	2.639+009	3.29	40.0	-.100-005	.236-006	2.619+009	3.27
20.0	-.100-006	.600-006	2.733+009	3.41	40.0	-.100-005	.600-006	2.898+009	3.62
20.0	-.100-006	.100-005	2.758+009	3.44	40.0	-.100-005	.100-005	2.980+009	3.72
20.0	-.236-006	.100-006	2.639+009	3.29					
20.0	-.236-006	.236-006	2.859+009	3.57					
20.0	-.236-006	.600-006	2.969+009	3.71					
20.0	-.236-006	.100-005	2.999+009	3.74					
20.0	-.600-006	.100-006	2.733+009	3.41					
20.0	-.600-006	.236-006	2.969+009	3.71					
20.0	-.600-006	.600-006	3.088+009	3.86					
20.0	-.600-006	.100-005	3.121+009	3.90					

TABLE 3(j)

$L = 700.$ $\alpha_1 = .236 \times 10^{-6}\ m^{-1}$

$Re(\theta) = .15 \times 10^{-1}$ Rad $Im(\theta) = .50 \times 10^{-3}$ Rad $Z_1 = 1000.$ m

DELM	α_2 (m^{-1})	α_3 (m^{-1})	FMAX (Hz)	ATNU (dB/km)	DELM	α_2 (m^{-1})	α_3 (m^{-1})	FMAX (Hz)	ATNU (dB/km)
10.0	-.100-006	.100-006	2.909+009	12.10	20.0	-.100-005	.100-006	2.751+009	11.45
10.0	-.100-006	.236-006	3.000+009	12.49	20.0	-.100-005	.236-006	2.993+009	12.46
10.0	-.100-006	.600-006	3.043+009	12.66	20.0	-.100-005	.600-006	3.115+009	12.96
10.0	-.100-006	.100-005	3.054+009	12.71	20.0	-.100-005	.100-005	3.149+009	13.10
10.0	-.236-006	.100-006	3.000+009	12.49	40.0	-.100-006	.100-006	1.682+009	7.00
10.0	-.236-006	.236-006	3.098+009	12.89	40.0	-.100-006	.236-006	1.954+009	8.13
10.0	-.236-006	.600-006	3.143+009	13.08	40.0	-.100-006	.600-006	2.106+009	8.76
10.0	-.236-006	.100-005	3.155+009	13.13	40.0	-.100-006	.100-005	2.149+009	8.94
10.0	-.600-006	.100-006	3.043+009	12.66	40.0	-.236-006	.100-006	1.954+009	8.13
10.0	-.600-006	.236-006	3.143+009	13.08	40.0	-.236-006	.236-006	2.331+009	9.70
10.0	-.600-006	.600-006	3.190+009	13.28	40.0	-.236-006	.600-006	2.550+009	10.61
10.0	-.600-006	.100-005	3.202+009	13.33	40.0	-.236-006	.100-005	2.614+009	10.88
10.0	-.100-005	.100-006	3.054+009	12.71	40.0	-.600-006	.100-006	2.106+009	8.76
10.0	-.100-005	.236-006	3.155+009	13.13	40.0	-.600-006	.236-006	2.550+009	10.61
10.0	-.100-005	.600-006	3.202+009	13.33	40.0	-.600-006	.600-006	2.815+009	11.71
10.0	-.100-005	.100-005	3.215+009	13.38	40.0	-.600-006	.100-005	2.893+009	12.04
20.0	-.100-006	.100-006	2.443+009	10.17	40.0	-.100-005	.100-006	2.149+009	8.94
20.0	-.100-006	.236-006	2.632+009	10.95	40.0	-.100-005	.236-006	2.614+009	10.88
20.0	-.100-006	.600-006	2.726+009	11.34	40.0	-.100-005	.600-006	2.893+009	12.04
20.0	-.100-006	.100-005	2.751+009	11.45	40.0	-.100-005	.100-005	2.975+009	12.38
20.0	-.236-006	.100-006	2.632+009	10.95					
20.0	-.236-006	.236-006	2.852+009	11.87					
20.0	-.236-006	.600-006	2.963+009	12.33					
20.0	-.236-006	.100-005	2.993+009	12.46					
20.0	-.600-006	.100-006	2.726+009	11.34					
20.0	-.600-006	.236-006	2.963+009	12.33					
20.0	-.600-006	.600-006	3.083+009	12.83					
20.0	-.600-006	.100-005	3.115+009	12.96					

TABLE 3(k)

L = 700. $\alpha_1 = .236 \times 10^{-6}\ m^{-1}$

$Re(\theta) = .15 \times 10^{-1}$ Rad $Im(\theta) = .15 \times 10^{-2}$ Rad $Z_1 = 1000.$ m

DELM	$\alpha_2\ (m^{-1})$	$\alpha_3\ (m^{-1})$	FMAX (Hz)	ATNU (dB/km)	DELM	$\alpha_2\ (m^{-1})$	$\alpha_3\ (m^{-1})$	FMAX (Hz)	ATNU (dB/km)
10.0	-.100-006	.100-006	2.539+009	31.70	20.0	-.100-005	.100-006	2.691+009	33.59
10.0	-.100-006	.236-006	2.931+009	36.60	20.0	-.100-005	.236-006	2.941+009	36.72
10.0	-.100-006	.600-006	2.978+009	37.18	20.0	-.100-005	.600-006	3.068+009	38.30
10.0	-.100-006	.100-005	2.991+009	37.34	20.0	-.100-005	.100-005	3.103+009	38.74
10.0	-.236-006	.100-006	2.931+009	36.60	40.0	-.100-006	.100-006	1.641+009	20.49
10.0	-.236-006	.236-006	3.039+009	37.94	40.0	-.100-006	.236-006	1.911+009	23.85
10.0	-.236-006	.600-006	3.089+009	38.57	40.0	-.100-006	.600-006	2.061+009	25.74
10.0	-.236-006	.100-005	3.103+009	38.74	40.0	-.100-006	.100-005	2.104+009	26.27
10.0	-.600-006	.100-006	2.978+009	37.18	40.0	-.236-006	.100-006	1.911+009	23.85
10.0	-.600-006	.236-006	3.089+009	38.57	40.0	-.236-006	.236-006	2.285+009	28.53
10.0	-.600-006	.600-006	3.142+009	39.22	40.0	-.236-006	.600-006	2.505+009	31.27
10.0	-.600-006	.100-005	3.155+009	39.40	40.0	-.236-006	.100-005	2.568+009	32.07
10.0	-.100-005	.100-006	2.991+009	37.34	40.0	-.600-006	.100-006	2.061+009	25.74
10.0	-.100-005	.236-006	3.103+009	38.74	40.0	-.600-006	.236-006	2.505+009	31.27
10.0	-.100-005	.600-006	3.155+009	39.40	40.0	-.600-006	.600-006	2.770+009	34.59
10.0	-.100-005	.100-005	3.169+009	39.57	40.0	-.600-006	.100-005	2.849+009	35.57
20.0	-.100-006	.100-006	2.375+009	29.66	40.0	-.100-005	.100-006	2.104+009	26.27
20.0	-.100-006	.236-006	2.568+009	32.06	40.0	-.100-005	.236-006	2.568+009	32.07
20.0	-.100-006	.600-006	2.665+009	33.27	40.0	-.100-005	.600-006	2.849+009	35.57
20.0	-.100-006	.100-005	2.691+009	33.59	40.0	-.100-005	.100-005	2.932+009	36.60
20.0	-.236-006	.100-006	2.568+009	32.06					
20.0	-.236-006	.236-006	2.795+009	34.89					
20.0	-.236-006	.600-006	2.910+009	36.33					
20.0	-.236-006	.100-005	2.941+009	36.72					
20.0	-.600-006	.100-006	2.665+009	33.27					
20.0	-.600-006	.236-006	2.910+009	36.33					
20.0	-.600-006	.600-006	3.034+009	37.88					
20.0	-.600-006	.100-005	3.068+009	38.30					

TABLE 3(b)

$L = 700.$ $\alpha_1 = .236 \times 10^{-6}\ m^{-1}$

$Re(\theta) = .15 \times 10^{-1}$ Rad $Im(\theta) = .50 \times 10^{-2}$ Rad $Z_1 = 1000.$ m

DELM	$\gamma_2\ (m^{-1})$	$\gamma_3\ (m^{-1})$	FMAX (Hz)	ATNU (dB/km)	DELM	$\gamma_2\ (m^{-1})$	$\gamma_3\ (m^{-1})$	FMAX (Hz)	ATNU (dB/km)
10.0	-.100-006	.100-006	7.668+008	31.91	20.0	-.100-005	.100-006	1.403+009	58.40
10.0	-.100-006	.236-006	1.055+009	43.91	20.0	-.100-005	.236-006	2.429+009	101.08
10.0	-.100-006	.600-006	1.268+009	52.75	20.0	-.100-005	.600-006	2.599+009	108.15
10.0	-.100-006	.100-005	1.337+009	55.66	20.0	-.100-005	.100-005	2.647+009	110.14
10.0	-.236-006	.100-006	1.055+009	43.91	40.0	-.100-006	.100-006	9.063+008	37.72
10.0	-.236-006	.236-006	1.691+009	70.36	40.0	-.100-006	.236-006	1.242+009	51.70
10.0	-.236-006	.600-006	2.312+009	96.21	40.0	-.100-006	.600-006	1.489+009	61.95
10.0	-.236-006	.100-005	2.555+009	106.34	40.0	-.100-006	.100-005	1.569+009	65.31
10.0	-.600-006	.100-006	1.268+009	52.75	40.0	-.236-006	.100-006	1.242+009	51.70
10.0	-.600-006	.236-006	2.312+009	96.21	40.0	-.236-006	.236-006	1.855+009	77.21
10.0	-.600-006	.600-006	2.652+009	110.39	40.0	-.236-006	.600-006	2.067+009	86.03
10.0	-.600-006	.100-005	2.681+009	111.58	40.0	-.236-006	.100-005	2.130+009	88.65
10.0	-.100-005	.100-006	1.337+009	55.66	40.0	-.600-006	.100-006	1.489+009	61.95
10.0	-.100-005	.236-006	2.555+009	106.34	40.0	-.600-006	.236-006	2.067+009	86.03
10.0	-.100-005	.600-006	2.681+009	111.58	40.0	-.600-006	.600-006	2.334+009	97.12
10.0	-.100-005	.100-005	2.710+009	112.79	40.0	-.600-006	.100-005	2.414+009	100.47
20.0	-.100-006	.100-006	8.062+008	33.55	40.0	-.100-005	.100-006	1.569+009	65.31
20.0	-.100-006	.236-006	1.108+009	46.12	40.0	-.100-005	.236-006	2.130+009	88.65
20.0	-.100-006	.600-006	1.330+009	55.37	40.0	-.100-005	.600-006	2.414+009	100.47
20.0	-.100-006	.100-005	1.403+009	58.40	40.0	-.100-005	.100-005	2.501+009	104.07
20.0	-.236-006	.100-006	1.108+009	46.12					
20.0	-.236-006	.236-006	1.772+009	73.73					
20.0	-.236-006	.600-006	2.388+009	99.40					
20.0	-.236-006	.100-005	2.429+009	101.08					
20.0	-.600-006	.100-006	1.330+009	55.37					
20.0	-.600-006	.236-006	2.388+009	99.40					
20.0	-.600-006	.600-006	2.552+009	106.22					
20.0	-.600-006	.100-005	2.599+009	108.15					

TABLE 3(m)

$L = 700.$ $\alpha_1 = .236 \times 10^{-6}\ m^{-1}$

$Re(\theta) = .15 \times 10^{-1}$ Rad $Im(\theta) = .15 \times 10^{-3}$ Rad $Z_1 = 1500.$ m

DELM	$\alpha_2\ (m^{-1})$	$\alpha_3\ (m^{-1})$	FMAX (Hz)	ATNU (dB/km)	DELM	$\alpha_2\ (m^{-1})$	$\alpha_3\ (m^{-1})$	FMAX (Hz)	ATNU (dB/km)
10.0	-.100-006	.100-006	1.668+009	2.08	20.0	-.100-005	.100-006	1.614+009	2.02
10.0	-.100-006	.236-006	1.697+009	2.12	20.0	-.100-005	.236-006	1.694+009	2.11
10.0	-.100-006	.600-006	1.710+009	2.14	20.0	-.100-005	.600-006	1.732+009	2.16
10.0	-.100-006	.100-005	1.714+009	2.14	20.0	-.100-005	.100-005	1.742+009	2.18
10.0	-.236-006	.100-006	1.697+009	2.12	40.0	-.100-006	.100-006	1.177+009	1.47
10.0	-.236-006	.236-006	1.727+009	2.16	40.0	-.100-006	.236-006	1.303+009	1.63
10.0	-.236-006	.600-006	1.741+009	2.17	40.0	-.100-006	.600-006	1.369+009	1.71
10.0	-.236-006	.100-005	1.744+009	2.18	40.0	-.100-006	.100-005	1.387+009	1.73
10.0	-.600-006	.100-006	1.710+009	2.14	40.0	-.236-006	.100-006	1.303+009	1.63
10.0	-.600-006	.236-006	1.741+009	2.17	40.0	-.236-006	.236-006	1.460+009	1.82
10.0	-.600-006	.600-006	1.755+009	2.19	40.0	-.236-006	.600-006	1.542+009	1.93
10.0	-.600-006	.100-005	1.758+009	2.20	40.0	-.236-006	.100-005	1.565+009	1.95
10.0	-.100-005	.100-006	1.714+009	2.14	40.0	-.600-006	.100-006	1.369+009	1.71
10.0	-.100-005	.236-006	1.744+009	2.18	40.0	-.600-006	.236-006	1.542+009	1.93
10.0	-.100-005	.600-006	1.758+009	2.20	40.0	-.600-006	.600-006	1.635+009	2.04
10.0	-.100-005	.100-005	1.762+009	2.20	40.0	-.600-006	.100-005	1.661+009	2.07
20.0	-.100-006	.100-006	1.504+009	1.88	40.0	-.100-005	.100-006	1.387+009	1.73
20.0	-.100-006	.236-006	1.573+009	1.96	40.0	-.100-005	.236-006	1.565+009	1.95
20.0	-.100-006	.600-006	1.605+009	2.00	40.0	-.100-005	.600-006	1.661+009	2.07
20.0	-.100-006	.100-005	1.614+009	2.02	40.0	-.100-005	.100-005	1.688+009	2.11
20.0	-.236-006	.100-006	1.573+009	1.96					
20.0	-.236-006	.236-006	1.648+009	2.06					
20.0	-.236-006	.600-006	1.684+009	2.10					
20.0	-.236-006	.100-005	1.694+009	2.11					
20.0	-.600-006	.100-006	1.605+009	2.00					
20.0	-.600-006	.236-006	1.684+009	2.10					
20.0	-.600-006	.600-006	1.722+009	2.15					
20.0	-.600-006	.100-005	1.732+009	2.16					

TABLE 3(n)

$L = 700.$ $\alpha_1 = .236 \times 10^{-6}\ m^{-1}$

$Re(\theta) = .15 \times 10^{-1}$ Rad $Im(\theta) = .50 \times 10^{-3}$ Rad $Z_1 = 1500.\ m$

DELM	$\alpha_2\ (m^{-1})$	$\alpha_3\ (m^{-1})$	FMAX (Hz)	ATNU (dB/km)	DELM	$\alpha_2\ (m^{-1})$	$\alpha_3\ (m^{-1})$	FMAX (Hz)	ATNU (dB/km)
10.0	-.100-006	.100-006	1.664+009	6.93	20.0	-.100-005	.100-006	1.611+009	6.71
10.0	-.100-006	.236-006	1.694+009	7.05	20.0	-.100-005	.236-006	1.692+009	7.04
10.0	-.100-006	.600-006	1.707+009	7.11	20.0	-.100-005	.600-006	1.730+009	7.20
10.0	-.100-006	.100-005	1.711+009	7.12	20.0	-.100-005	.100-005	1.740+009	7.24
10.0	-.236-006	.100-006	1.694+009	7.05	40.0	-.100-006	.100-006	1.174+009	4.89
10.0	-.236-006	.236-006	1.725+009	7.18	40.0	-.100-006	.236-006	1.301+009	5.41
10.0	-.236-006	.600-006	1.739+009	7.24	40.0	-.100-006	.600-006	1.366+009	5.69
10.0	-.236-006	.100-005	1.742+009	7.25	40.0	-.100-006	.100-005	1.384+009	5.76
10.0	-.600-006	.100-006	1.707+009	7.11	40.0	-.236-006	.100-006	1.301+009	5.41
10.0	-.600-006	.236-006	1.739+009	7.24	40.0	-.236-006	.236-006	1.457+009	6.07
10.0	-.600-006	.600-006	1.753+009	7.29	40.0	-.236-006	.600-006	1.540+009	6.41
10.0	-.600-006	.100-005	1.757+009	7.31	40.0	-.236-006	.100-005	1.563+009	6.51
10.0	-.100-005	.100-006	1.711+009	7.12	40.0	-.600-006	.100-006	1.366+009	5.69
10.0	-.100-005	.236-006	1.742+009	7.25	40.0	-.600-006	.236-006	1.540+009	6.41
10.0	-.100-005	.600-006	1.757+009	7.31	40.0	-.600-006	.600-006	1.633+009	6.80
10.0	-.100-005	.100-005	1.760+009	7.33	40.0	-.600-006	.100-005	1.659+009	6.90
20.0	-.100-006	.100-006	1.501+009	6.24	40.0	-.100-005	.100-006	1.384+009	5.76
20.0	-.100-006	.236-006	1.570+009	6.53	40.0	-.100-005	.236-006	1.563+009	6.51
20.0	-.100-006	.600-006	1.603+009	6.67	40.0	-.100-005	.600-006	1.659+009	6.90
20.0	-.100-006	.100-005	1.611+009	6.71	40.0	-.100-005	.100-005	1.686+009	7.02
20.0	-.236-006	.100-006	1.570+009	6.53					
20.0	-.236-006	.236-006	1.646+009	6.85					
20.0	-.236-006	.600-006	1.682+009	7.00					
20.0	-.236-006	.100-005	1.692+009	7.04					
20.0	-.600-006	.100-006	1.603+009	6.67					
20.0	-.600-006	.236-006	1.682+009	7.00					
20.0	-.600-006	.600-006	1.720+009	7.16					
20.0	-.600-006	.100-005	1.730+009	7.20					

TABLE 3(o)

$L = 700.$ $\alpha_1 = .236 \times 10^{-6}\ m^{-1}$

$Re(\theta) = .15 \times 10^{-1}$ Rad $Im(\theta) = .15 \times 10^{-2}$ Rad $Z_1 = 1500.$ m

DELM	α_2 (m^{-1})	α_3 (m^{-1})	FMAX (Hz)	ATNU (dB/km)	DELM	α_2 (m^{-1})	α_3 (m^{-1})	FMAX (Hz)	ATNU (dB/km)
10.0	-.100-006	.100-006	1.636+009	20.43	20.0	-.100-005	.100-006	1.588+009	19.83
10.0	-.100-006	.236-006	1.669+009	20.84	20.0	-.100-005	.236-006	1.672+009	20.88
10.0	-.100-006	.600-006	1.684+009	21.03	20.0	-.100-005	.600-006	1.713+009	21.38
10.0	-.100-006	.100-005	1.688+009	21.08	20.0	-.100-005	.100-005	1.724+009	21.52
10.0	-.236-006	.100-006	1.669+009	20.84	40.0	-.100-006	.100-006	1.153+009	14.40
10.0	-.236-006	.236-006	1.704+009	21.27	40.0	-.100-006	.236-006	1.280+009	15.98
10.0	-.236-006	.600-006	1.719+009	21.47	40.0	-.100-006	.600-006	1.346+009	16.80
10.0	-.236-006	.100-005	1.724+009	21.52	40.0	-.100-006	.100-005	1.364+009	17.03
10.0	-.600-006	.100-006	1.684+009	21.03	40.0	-.236-006	.100-006	1.280+009	15.98
10.0	-.600-006	.236-006	1.719+009	21.47	40.0	-.236-006	.236-006	1.438+009	17.95
10.0	-.600-006	.600-006	1.735+009	21.67	40.0	-.236-006	.600-006	1.522+009	19.00
10.0	-.600-006	.100-005	1.740+009	21.72	40.0	-.236-006	.100-005	1.545+009	19.29
10.0	-.100-005	.100-006	1.688+009	21.08	40.0	-.600-006	.100-006	1.346+009	16.80
10.0	-.100-005	.236-006	1.724+009	21.52	40.0	-.600-006	.236-006	1.522+009	19.00
10.0	-.100-005	.600-006	1.740+009	21.72	40.0	-.600-006	.600-006	1.616+009	20.17
10.0	-.100-005	.100-005	1.744+009	21.77	40.0	-.600-006	.100-005	1.642+009	20.50
20.0	-.100-006	.100-006	1.473+009	18.39	40.0	-.100-005	.100-006	1.364+009	17.03
20.0	-.100-006	.236-006	1.545+009	19.29	40.0	-.100-005	.236-006	1.545+009	19.29
20.0	-.100-006	.600-006	1.579+009	19.72	40.0	-.100-005	.600-006	1.642+009	20.50
20.0	-.100-006	.100-005	1.588+009	19.83	40.0	-.100-005	.100-005	1.669+009	20.84
20.0	-.236-006	.100-006	1.545+009	19.29					
20.0	-.236-006	.236-006	1.624+009	20.28					
20.0	-.236-006	.600-006	1.662+009	20.75					
20.0	-.236-006	.100-005	1.672+009	20.88					
20.0	-.600-006	.100-006	1.579+009	19.72					
20.0	-.600-006	.236-006	1.662+009	20.75					
20.0	-.600-006	.600-006	1.702+009	21.25					
20.0	-.600-006	.100-005	1.713+009	21.38					

TABLE 3(p)

$L = 700.$ $\alpha_1 = .236 \times 10^{-6}\ m^{-1}$

$Re(\theta) = 1.5 \times 10^{-1}$ Rad $Im(\theta) = .50 \times 10^{-2}$ Rad $Z_1 = 1500.$ m

DELM	$\alpha_2\ (m^{-1})$	$\alpha_3\ (m^{-1})$	FMAX (Hz)	ATNU (dB/km)	DELM	$\alpha_2\ (m^{-1})$	$\alpha_3\ (m^{-1})$	FMAX (Hz)	ATNU (dB/km)
10.0	-.100-006	.100-006	7.440+008	30.96	20.0	-.100-005	.100-006	1.329+009	55.31
10.0	-.100-006	.236-006	1.012+009	42.13	20.0	-.100-005	.236-006	1.472+009	61.26
10.0	-.100-006	.600-006	1.207+009	50.21	20.0	-.100-005	.600-006	1.533+009	63.78
10.0	-.100-006	.100-005	1.270+009	52.84	20.0	-.100-005	.100-005	1.549+009	64.47
10.0	-.236-006	.100-006	1.012+009	42.13	40.0	-.100-006	.100-006	8.746+008	36.40
10.0	-.236-006	.236-006	1.480+009	61.60	40.0	-.100-006	.236-006	1.075+009	44.73
10.0	-.236-006	.600-006	1.515+009	63.04	40.0	-.100-006	.600-006	1.143+009	47.55
10.0	-.236-006	.100-005	1.524+009	63.43	40.0	-.100-006	.100-005	1.162+009	48.34
10.0	-.600-006	.100-006	1.207+009	50.21	40.0	-.236-006	.100-006	1.075+009	44.73
10.0	-.600-006	.236-006	1.515+009	63.04	40.0	-.236-006	.236-006	1.240+009	51.59
10.0	-.600-006	.600-006	1.551+009	64.56	40.0	-.236-006	.600-006	1.331+009	55.38
10.0	-.600-006	.100-005	1.561+009	64.96	40.0	-.236-006	.100-005	1.357+009	56.46
10.0	-.100-005	.100-006	1.270+009	52.84	40.0	-.600-006	.100-006	1.143+009	47.55
10.0	-.100-005	.236-006	1.524+009	63.43	40.0	-.600-006	.236-006	1.331+009	55.38
10.0	-.100-005	.600-006	1.561+009	64.96	40.0	-.600-006	.600-006	1.436+009	59.78
10.0	-.100-005	.100-005	1.571+009	65.37	40.0	-.600-006	.100-005	1.467+009	61.03
20.0	-.100-006	.100-006	7.811+008	32.51	40.0	-.100-005	.100-006	1.162+009	48.34
20.0	-.100-006	.236-006	1.061+009	44.16	40.0	-.100-005	.236-006	1.357+009	56.46
20.0	-.100-006	.600-006	1.263+009	52.57	40.0	-.100-005	.600-006	1.467+009	61.03
20.0	-.100-006	.100-005	1.329+009	55.31	40.0	-.100-005	.100-005	1.498+009	62.34
20.0	-.236-006	.100-006	1.061+009	44.16					
20.0	-.236-006	.236-006	1.402+009	58.35					
20.0	-.236-006	.600-006	1.457+009	60.64					
20.0	-.236-006	.100-005	1.472+009	61.26					
20.0	-.600-006	.100-006	1.263+009	52.57					
20.0	-.600-006	.236-006	1.457+009	60.64					
20.0	-.600-006	.600-006	1.516+009	63.11					
20.0	-.600-006	.100-005	1.533+009	63.78					

7. CONCLUSIONS

To use the RFM as a search scheme for modal solutions, the original modal equation (equation 3) expressed in terms of plane wave reflection coefficients $R_D(\theta)$ and $\bar{R}_D(\theta)$ was modified in such a way as to effectively move its poles to the point infinity in the complex plane. One reason for this modification is clearly depicted in figures 10 and 11. Figure 10 exhibits "phase line extinction" associated with poles which occur within the search rectangle. "Phase line extinction" makes it possible for the RFM to miss solutions within the search rectangle. Figure 11 shows the much relaxed phase contour structure which results with all poles moved to the point infinity. For such phase contour behavior, the RFM will pick up all modes within the search rectangle. The modification of the original modal equation has one serious disadvantage in the sense that numerically large factors occurring in the numerators and demoninators of quantities which occur in the original mode equation and which can be simply canceled out in the ratio, occur as products, rather than ratios, in the modified modal equation. This disadvantage can result in overflow problems in the microwave range.

For the case study of the trilinear layer of figure 8, implementation of a single precision version of the RFM on a Univac 1110 was straightforward and successful for the 65-, 170-, and 520-MHz cases examined. Figure 9 is a representation of the RFM applied to the 520-MHz case, this being an interesting example of this lower frequency domain. Figure 9 illustrates the interesting feature that the RFM does not necessarily locate roots sequentially according to the magnitude of $\mathrm{Re}(\theta)$.

Overflow was a problem for the 3.3-GHz case, although it would not have been had a double precision version of the RFM been used. Function switching (see section 5) and search rectangle subdivision (see section 6) have been utilized to overcome the overflow problems in this case in such a way that computer run times were comparable with those of the more conventional Newton-Raphson scheme. Unlike the latter, of course, the RFM assures the location of all zeros (or modes) within the search rectangle.

Unfortunately, function switching along with search rectangle subdivision is very difficult to automate (this would be especially true for multisegmented profiles). Thus, the RFM appears to have its greatest utility for tropospheric propagation when function switching and search rectangle subdivision can be altogether avoided. For this reason a set of tables (tables 3(a) through 3(p)) has been prepared as a guide to the waveguide program user. The tables show an estimated maximum frequency, FMAX, below which function switching should not occur for several trilinear layer models and various search rectangles. The method of calculation should assure a rather conservative estimate of FMAX (ie, switching should not occur until frequencies somewhat higher than FMAX are encountered). Since there are many practical instances when FMAX is on the order of 5 GHz or more, we recommend implementing the RFM with a multisegmented waveguide model.

REFERENCES

1. Wait, JR, and Spies, KP, Internal guiding of microwaves by an elevated tropospheric layer, Radio Sci, vol 4, 1969, p 319–326

2. Chang, HT, The effect of tropospheric layer structures on long range VHF radio propagation, IEEE Trans Antennas Propagat, AP19, p 751–756

3. Dresp, MR, Radio wave propagation in the presence of an elevated tropospheric duct, PhD Thesis (1972) University of Pennsylvania, Philadelphia, Pennsylvania

4. Dresp, MK, Tropospheric duct propagation at VHF, UHF and SHF, Mitre Corporation Technical Report MTR-3114, vol 1, October 1975

5. Pappert, RA, and Goodhart, CL, Case studies of beyond-the-horizon propagation in tropospheric ducting environments, Radio Sci, vol 12, 1977, p 75–87

6. Cho, SH, and Wait, JR, EM wave propagation in a laterally nonuniform troposphere, Cooperative Institute for Research in Environmental Sciences (CIRES), University of Colorado, EM Report 1, June 15, 1977, p 142

7. Hamming, RW, Numerical Methods for Scientists and Engineers, (second edition), McGraw-Hill, New York, 1973

8. Morfitt, DG, and Shellman, CH, "MODESRCH" an improved computer program for obtaining ELF/VLF/LF mode constants in an earth-ionosphere waveguide, Naval Electronics Laboratory Center interim report 77T prepared for the Defense Nuclear Agency (DNA), 1 October 1976

9. Computation Laboratory, Tables of the Modified Hankel Functions of Order One Third and Their Directives, Harvard University Press, Cambridge, Massachusetts, 1945

10. Churchill, RV, Brown, JW and Verley, RF, Complex Variables and Applications (third edition), McGraw-Hill, New York, 1974, p 296

11. Pappert, R, Goodhart, C, Waveguide calculation of signal levels in tropospheric ducting environments, Naval Electronics Laboratory Center TN 3129, February 1976

APPENDIX A: DERIVATION OF THE POLE-FREE CONTINUOUS VERSION OF THE MODAL EQUATION

A pole-free discontinuous version of the modal equation is given by equations (24) through (27) of section 5. In this appendix we sketch the derivation of the pole-free continuous version given by equations (28) through (31) of section 5. The essence of the derivation depends upon the asymptotic behavior of the denominators DZ2, DA2, and DB1 given by equations (4), (5), and (17) of section 5 since the switching from one function to another occurs only if the imaginary part of one or all of the quantities $p_3(1)$, $p_2(2)$, and $p_1(1)$ is sufficiently large (as determined by L in the inequality (23)). Furthermore, we also know from the physics of the problem that $\mathrm{Im}\,(p_3(1), p_2(2), p_1(1)) > 0$. It is assumed that the switch from one function to the other occurs only when the modified refractive index is sufficiently negative. Mathematically this condition is formulated by requiring that the relevant quantity or quantities, $\mathrm{Arg}\,(p_3(1))$, $\mathrm{Arg}\,(p_2(2))$, $\mathrm{Arg}\,(p_1(1))$ be greater than $2/3\,\pi$. Thus, summarizing to this point, we are concerned with the asymptotic development of the denominators DZ2, DA2, and DB1 in the region of the complex plane bounded by the radial $2/3\,\pi$ and the negative real axis. The appropriate asymptotic expansions of the modified Hankel function of order one-third are therefore:

$$h_1(q) \sim \beta\, q^{-1/4} \exp\left(\frac{2}{3} i\, q^{3/2} - \frac{5}{12}\pi i\right) \tag{A.1}$$

$$h_1'(1) \sim i\beta\, q^{1/4} \exp\left(\frac{2}{3} i\, q^{3/2} - \frac{5}{12}\pi i\right) \tag{A.2}$$

$$h_2(q) \sim \beta\, q^{-1/4} \exp\left(\frac{2}{3} i\, q^{3/2} + \frac{11}{12}\pi i\right) \tag{A.3}$$

$$h_2'(q) \sim i\beta\, q^{1/4} \exp\left(\frac{2}{3} i\, q^{3/2} + \frac{11}{12}\pi i\right) \tag{A.4}$$

From these formulas, the asymptotic developments of the denominators DZ2, DA2, and DB1 given by equations (4), (5), and (17) of section 5 are:

$$DZ2 \sim i\beta\,(p_1(3))^{1/4} \exp\left(\frac{2}{3} i\,(p_1(3))^{3/2} + \frac{11}{12}\pi i\right) \tag{A.5}$$

$$DA2 \sim 2\beta\,(p_2(2))^{-1/4} \exp\left(\frac{2}{3} i\,(p_2(2))^{3/2} - \frac{5}{12}\pi i\right) \tag{A.6}$$

$$DB1 \sim \beta\,(p_1(1))^{-1/4}\left(1 - \varepsilon_0\,(s^2 - \alpha_1 H)^{1/2}\right) \exp\left(\frac{2}{3} i (p_1(1))^{3/2} - \frac{5}{12}\pi i\right) \tag{A.7}$$

Now observe that F_1 given by equation (24) of section 5, differs from F_4 given by equation (27) by the factors DZ2 × DA2 × DZ0 × DB1. Thus, one way they can be made continuous at the switching boundary is to multiply F_1 by

$$(DZ2)^{-1} \times (DA2)^{-1} \times (DB1)^{-1} \tag{A.8}$$

where the denominators are the asymptotic expressions given in equations (A.5) through (A.7) and to multiply F_4 by DZ0. Next F_2 as given by Equation (25) of section 5 can be made continuous at the switching boundary with this newly formed F_4 by multiplying the F_2 by $(DB1)^{-1}$. Similarly, F_3 given by equation (26) of section 5 can be made continuous

with the newly formed F_4 at the switching boundary by multiplying F_3 by $(DZ2)^{-1} \times (DA2)^{-1}$. Finally, the M_i's given in equations (28) through (31) of section 5 are obtained by multiplying the new set of F_i's through by the factor, $(p_1(1))^{-1/4}(1-s_0(S^2 - \alpha_1 H)^{1/2})$.